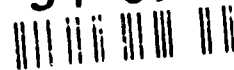


AD-A276 630



DTIC
S-10

94-07237



DTIC QUALITY INSPECTED 1

94 8 08 179

INDEX

TEXT	PAGE NO
DD 1473	1
Title Page	2
Abstract	3
1. Introduction	4
2. Theory of Sinusoidal Transmission Grating	4
3. Experimental	5
4.0 Results & Discussion	6
4.1 Single Sinusoidal Transmission Gratings (made by NPL)	6
4.2 Groove Depth Determination By SEM Technique	7
4.3 Crossed Gratings On Different Substrates (NPL)	7
4.4 Crossed Grating System On A Single Substrate (NPL)	7
4.5 Optometrics (U.K.) Single Sinusoidal Gratings	8
5. Principles of Multilayer Dielectric Thin Film Mirrors (i.e. Filters)	9
5.1 Results and Discussions: Dielectric Mirrors	11
5.2 Conclusion	13
6. References	13

TABLE:

Table 1:	Estimated Values of Physical Groove Depths a', of NPL Sinusoidal Gratings	14
----------	--	----

FIGURES:

Figure 1:	Sinusoidal transmission phase grating	15
Figure 2:	Distortion of plane wave due to grating profile	16

(1)

Accession For	
15 NTIS GRA&I	<input checked="" type="checkbox"/>
DTIC TAB	<input type="checkbox"/>
Unannounced	<input type="checkbox"/>
16 Justification	
By _____	
Distribution/ _____	
Availability Codes	
Dist	Avail and/or Special
A-1	

Figure 3:	Zero and first order diffraction efficiencies of a sine-wave phase grating (amplitude a' medium refractive index n_0), as calculated from equation 4	17
Figure 4:	Section of a holographically produced, single profile, sinusoidal phase diffraction grating	18
Figure 5:	Two sections of a holographically produced, crossed profile, sinusoidal phase diffraction grating	19
Figure 6:	Wavelength response experimental arrangement	20
Figure 7:	Power spectrum of the light source	21
Figure 8:	Normalized transmittance (%) wavelength (nm) of gratings 1 of groove depth 637nm	22
Figure 9:	Normalized transmittance (%) wavelength (nm) of grating 2 of groove depth 647nm	23
Figure 10:	Normalized transmittance (%) wavelength (nm) of grating 3 of groove depth 657nm	24
Figure 11:	Normalized transmittance (%) wavelength (nm) of grating 4 of groove depth 667nm	25
Figure 12:	Normalized transmittance (%) wavelength (nm) of grating 5 of groove depth 677nm	26
Figure 13:	Normalized transmittance (%) wavelength (nm) of grating 6 of groove depth 696nm	27

Figure 14:	Normalized transmittance (%) wavelength (nm) of grating 7 of groove depth 706nm	28
Figure 15:	Normalized transmittance (%) wavelength (nm) of grating 7 of groove depth 737nm	29
Figure 16:	Normalized transmittance (%) wavelength (nm) of grating 9 of wavelength 771nm	30
Figure 17:	Normalized transmittance (%) wavelength (nm) of grating 10 of groove depth 776nm	31
Figure 18:	Behaviour of the physical groove depth a' and λ_{\min} in at which the minimum transmittance occurs	32
Figure 19:	SEM shadow casting in determining the groove depth of NPL grating 10	33
Figure 20:	Normalized transmittance (%) wavelength (nm) for gratings 10 (776nm groove depth) and 1 (637nm groove depth) placed crosswise	34
Figure 21:	Crossed sinusoidal photo-resist grating 11 on a glass substrate, 600 lines/mm, groove depth ~ 896nm (estimated)	35
Figure 22:	Normalized transmittance (%) wavelength (nm) of grating 13 (optometrics) of groove depth 537nm	36
Figure 23:	Simplified function of all dielectric reflector	37

Figure 24:	Computed spectral reflectance of periodic quarterwave layer reflector of ZnS ($n_H = 2.35$) and magnesium fluoride ($n_L = 1.38$) deposited on glass ($n_s = 1.52$). $n_o = 1.00$. Full curve, three layers; broken curve, five layers; dotted curve, nine layers.	38
Figure 25:	Spectral response of a dielectric mirror deposited on an uncoated glass substrate.	39
Figure 26:	Spectral response of a dielectric mirror deposited on an uncoated glass substrate.	40
Figure 27:	Normalized transmittance of optical filter on Polycarbonate substrate.	41
Figure 28:	Normalized transmittance (at different incident angles) of optical filter on Polycarbonate substrate.	42
Figure 29:	Transmission characteristic of Notch and Block filter at normal incidence (two polycarbonate substrates, sandwiched together with no UV curing glue).	43
Figure 30:	Transmission Characteristic of a dielectric mirror deposited on one surface of a polycarbonate substrate (size: 50mm x 50mm x 3mm).	44

Unclassified
 SECURITY CLASSIFICATION OF THIS PAGE

REPORT DOCUMENTATION PAGE

1. REPORT SECURITY CLASSIFICATION Unclassified		1b. RESTRICTIVE MARKINGS	
2a. SECURITY CLASSIFICATION AUTHORITY		3. DISTRIBUTION / AVAILABILITY OF REPORT Approved for public release; distribution unlimited	
2b. DECLASSIFICATION / DOWNGRADING SCHEDULE			
4. PERFORMING ORGANIZATION REPORT NUMBER(S)		5. MONITORING ORGANIZATION REPORT NUMBER(S) R&D 6310-MS-01	
6a. NAME OF PERFORMING ORGANIZATION University College of North Wales	6b. OFFICE SYMBOL (if applicable)	7a. NAME OF MONITORING ORGANIZATION European Research Office USARDSG-UK	
6c. ADDRESS (City, State, and ZIP Code) College Road, Bangor, Gwynedd, LL57 2DG Wales, UK		7b. ADDRESS (City, State, and ZIP Code) PSC 802 Box 15 FPO AE 09499-1500	
8a. NAME OF FUNDING / SPONSORING ORGANIZATION EUROPEAN Research Office USARDSG-UK ARNLS	8b. OFFICE SYMBOL (if applicable)	9. PROCUREMENT INSTRUMENT IDENTIFICATION NUMBER DAJA45-90-C-0005	
8c. ADDRESS (City, State, and ZIP Code) PSC 802 Box 15 FPO AE 09499-1500		10. SOURCE OF FUNDING NUMBERS	
		PROGRAM ELEMENT NO. 0601102A	PROJECT NO. 1L161102BH57
		TASK NO. 04	WORK UNIT ACCESSION NO.

TITLE (Include Security Classification)

(U) Optical Beam Deflection System

PERSONAL AUTHOR(S)
Dr. D.K. Das-Gudra

13a. TYPE OF REPORT Final	13b. TIME COVERED FROM Dec 89 TO Feb 93	14. DATE OF REPORT (Year, Month, Day) 1993 June 18	15. PAGE COUNT Fourteen
------------------------------	--	---	----------------------------

SUPPLEMENTARY NOTATION

COSATI CODES			18. SUBJECT TERMS (Continue on reverse if necessary and identify by block number)
FIELD	GROUP	SUB-GROUP	
1705			
2006			

19. ABSTRACT (Continue on reverse if necessary and identify by block number)

The transmission spectra in the wavelength range of 400nm to 1000nm have been studied with (i) sinusoidal phase transmission gratings formed on photo-resist materials on glass substrates and (ii) dielectric mirrors (filters) formed by depositing multiple and alternate layers of 'High' and 'Low' inorganic dielectric materials on glass and polycarbonate substrates.

With the sinusoidal crossed two groove profiles transmission gratings of groove depth ~ 896nm on a single substrate a transmission was of less than 1% at 500-680nm and the transmittance did not exceed 12% over the entire range of 400-1000nm. The transmission over the visible part of the wavelength was poor although the gratings satisfied the required specification.

The multiple layer all dielectric mirror, produced on one surface of a polycarbonate substrate (50mmx50mmx3mm) satisfied the following specification: (i) <0.5% transmission at 532nm, (ii) <1.0% transmission from 694nm, (iii) 50% transmission from 400nm to 500nm and from 560nm to 600nm. The performance mentioned above satisfied adequately the required specification.

20. DISTRIBUTION / AVAILABILITY OF ABSTRACT <input checked="" type="checkbox"/> UNCLASSIFIED/UNLIMITED <input checked="" type="checkbox"/> SAME AS RPT. <input checked="" type="checkbox"/> DTIC USERS		21. ABSTRACT SECURITY CLASSIFICATION Unclassified	
22a. NAME OF RESPONSIBLE INDIVIDUAL		22b. TELEPHONE (Include Area Code) 071 409 4423	22c. OFFICE SYMBOL AMXSN-UK-RM

DAJA45-90-C-0005

FAST ACTING OPTICAL DEFLECTION

FINAL REPORT
(JUNE 1993)

A.K. Das-Gupta
School of Electronic Engineering and Computer Science
University of Wales, Bangor
Dean Street, Bangor
Gwynedd, LL57 1UT, UK

Telephone: (0248) 382696
Fax: (0248) 361429

Abstract

The present work is primarily concerned with the investigation of the spectral transmittance of sinusoidal phase transmission gratings of coherent radiations in order to obtain minimum transmission in the wavelength range of ~ 0.5 micron to 1 micron. The zero order transmittance of fourteen sinusoidal transmission gratings with 600 lines per mm have been measured. All the gratings were formed on photo-resist materials on glass substrates using a holographic technique. Ten gratings of varying groove depths in the range of $\sim 637\text{nm}$ to 776nm were provided by the National Physical Laboratory (NPL) of the United Kingdom. NPL also produced two further gratings in which the two sinusoidal corrugations were superimposed (i.e. 90° to each other, the crossed grating), on a single glass substrate, the effective groove depth being $\sim 896\text{nm}$. The remaining two gratings of groove depth $\sim 537\text{nm}$ were obtained from the Optometrics (U.K.) Limited.

The transmission spectrum was found to be a function of the groove depth only, the diffraction angle being determined by the grating period. A high degree attenuation of the zero order beam over a small wavelength region is attainable with a single sinusoidal transmission grating of appropriate groove depth. The deeper the peak to peak amplitude of the sinusoidal profile is, the higher is the value of λ_{min} , at which the transmittance is minimum.

The gratings can be combined by linear superposition of their characteristics. Using two separate gratings of dissimilar groove depths of 637nm and 776nm and with profiles at right angles to each other, a maximum of 6% transmittance was obtained for the zero order beam over a spectral range of $400\text{-}1000\text{nm}$, λ_{min} being at $\sim 565\text{nm}$. A crossed two groove profiles normal to each other) with a groove depth of $\sim 896\text{nm}$ on a single substrate provided less than 1% transmittance at $500\text{-}680\text{nm}$ wavelength and the transmittance did not exceed 12% for the entire band of $400\text{-}1000\text{nm}$.

The crossed gratings format described above, satisfied the required specification. However, the transmittance in the visible part of the spectrum, with deep groove depth, is very low.

To overcome the difficulty mentioned above and to cope with a new specification which required a good transmission, i.e. $\sim 50\%$ transmission in the visible region of spectrum and that the transmission should be as little as possible in the wavelength region $>650\text{nm} - 1000\text{nm}$ multilayer all dielectric mirrors were fabricated on polycarbonate substrates.

The final effort was to produce such a mirror on a single surface of a polycarbonate substrate ($50\text{mm} \times 50\text{mm} \times 3\text{mm}$) which has the following specifications:

- (i) $<0.5\%$ transmission at 532nm .
- (ii) $<1.0\%$ transmission from 694nm to 1064nm
- (iii) 50% transmission from 400 to 500nm and from 560nm to 600nm .

The performances mentioned above, satisfy the requirements which were expected in this work.

1. Introduction

The objective of the present work has been a study of the behaviour of the deflection of coherent laser radiations in the wavelength range of 0.400 microns to 1.000 microns using (i) Sinusoidal Transmission Grating with appropriate groove depths and (ii) Multilayer All Dielectric Films containing alternate high and low refractive indices.

The optical transmission of a combination of two sinusoidal gratings of suitable groove depths, prepared by a photoresist technique, has been studied. In this arrangement the plane of corrugation of one grating is located perpendicular to the other in order to obtain a maximum attenuation of the zeroth order beam in the spectral range stated above. The transmission spectra has also been studied with a single glass substrate on which two separate grooves, normal to each other, were introduced.

The multilayer dielectric mirrors were successfully employed to obtain both stop bands and pass bands on glass and polycarbonate substrates for which the spectral transmission requirements have been stringent.

The present report provides a brief description of the optical behaviour of both the techniques (i.e. sinusoidal transmission gratings and the multilayer all dielectric mirror, together with the results). The latter method shows considerable promise in the field of laser radiation protection technology.

2. Theory of Sinusoidal Transmission Grating

Figure 1 shows the general profile of the sinusoidal transmission phase grating. The grating corrugations have a period d and physical groove depth a' . A characteristic feature of the sinusoidal transmission grating is the low intensity of the even diffraction order m ($m = 2, 4, 6$ etc). This fact ensures their stability for multiple imaging applications [1]. The diffraction angle β is given by the familiar grating equation (see figure 1).

$$d \sin \beta_m = m\lambda \quad \dots (1)$$

where λ is the wavelength of the incident coherent radiation. Note that the diffraction angle is dependent on the ratio λ/d only and not on the structure of the grating. The diffraction pattern produced by a sinusoidal transmission grating, however, depends on the actual profile of the grating. The wavefront is distorted (see figure 2) due to the velocities of the waves in the different media. The diffraction efficiency of a sinusoidal grating of refractive index n_g in air is given by [1-3].

$$D_m = \left[\left(\frac{1}{d} \right) \int_0^d \left(\exp 2\pi i s(x) (n_g - 1)/\lambda - \frac{mx}{d} \right) dx \right]^2 \quad \dots (2)$$

where D is the diffraction efficiency. $s(x)$ represents a relief function of the grating. The factor $1/d$ provides a normalization.

With the sinusoidal gratings,

$$s(x) = \frac{a'}{2} \sin \left(\frac{2\pi x}{d} \right) \quad \dots (3)$$

Substituting equation 3 in equation 2, we get [2, 3],

$$D_1 = J_1^2 \left[\pi a' (n_g - 1) \lambda \right] \quad \dots (4)$$

where J_1 is the first order Bessel function of the first kind. Thus the diffraction efficiency of a sinusoidal grating takes the form of a squared Bessel function. This function has been plotted in figure 3 for the zero and the first order beams.

3. Experimental

Ten sinusoidal (phase) gratings of different, but unspecified groove depths, formed on photo-resist (refractive index $n_g = 1.64$ at 634nm) on glass substrates ($n_s = 1.46$ at 635nm) were provided by the National Physical Laboratories, (NPL), U.K. These gratings were produced by the NPL using a holographic technique.

The gratings specifications are as follows:

600 lines per mm sinusoidal photo resist gratings on 30mm diameter green plate glass with various groove depths from ~ 637 to 776 nm.

The actual groove depth a' was not specified by the NPL, but estimated in the present work.

The NPL also provided two holographically produced crossed sinusoidal (phase) diffraction gratings using similar photoresist and substrate materials, stated above, the groove period being again 600 lines per mm. the groove depths were unspecified. Figure 4 and 5 show schematically sections of single profile and crossed profile sinusoidal phase gratings.

Two other single profile holographically produced sinusoidal photoresist gratings (600 lines per mm) on 25.4 mm² glass plate were provided by Optometrics (UK) Ltd. The groove depths of these two gratings were again not specified by the manufacturer.

The transmission spectra of all these gratings were studied in our laboratories using a well focused microscope lamp (light source), a monochromator (Hilger and Watts) and a silicon photo detector (Anritsu Model ML9002A Power Meter with Model MA 9422A Sensor). A schematic diagram of the experimental arrangement is shown figure 6. Measurements of the transmission spectra were made over the range of wavelengths from 400nm to 1000nm in steps of 25nm using the calibrated monochromator. The transmission spectral data for each grating were normalized with respect to the power spectrum of the light source in the same wavelength region.

4.0 Results & Discussion

4.1 Single Sinusoidal Transmission Gratings (NPL)

Figure 7 shows the power spectrum of the light source used in the present work. The normalized transmittance (%) spectra of the ten NPL sinusoidal gratings in the wavelength range of 400-1000 nm are shown in figures 8-17. It should be noted that the stated groove depth in figures 8-17 refer to the physical peak to peak value a' , estimated from the spectral response in each case.

The optical peak to peak amplitude a is related to the physical peak to peak value a' of the groove thus,

$$a = a' (n_g - n_a) \quad \dots\dots (5)$$

where n_g and n_a are the refractive indices of grating medium and air respectively. Thus, higher the difference in the refractive indices is, the smaller is the physical amplitude a' of the groove of the grating for a given response. This is an advantage, in general, as the quality of the profile tends to deteriorate with increasing depth during the fabrication of the grating. However, refractive indices of most epoxies, plastics and glasses are in the range 1.4 to 1.7, although special glasses with the refractive index of 2.4 do exist. It is, however, difficult to have deep etching with hard glass.

The groove depth may be estimated by assuming that the zero order transmittance to be zero at a wavelength where it is observed to be a minimum. Thus we may write from equations 4 and 5,

$$0 = J_0^2 \left[\pi a^1 \left(n_g - n_a \right) / \lambda \right] \quad \dots\dots (6)$$

By a reference to a table of Bessel functions [4] the value of J_0^2 at which the transmittance is zero, is found to be 2.4. Equation 6 may be solved and with $n_g = 1.64$ and $n_a = 1$ and we get,

$$a^1 = 1.19 \lambda_{\min} \quad \dots\dots (7)$$

where λ_{\min} is the wavelength at which minimum transmittance occurs. The magnitude of the physical peak to peak groove depth may be estimated from the experimental observation of λ at which the transmittance is a minimum (i.e., λ_{\min}).

Using the above analysis a' - values of the ten NPL gratings were calculated from the λ_{\min} - values in figures 8-17.

Table 1 and figure 18 show the behaviour of λ_{\min} and the a' - values (peak to peak physical groove depth) from which it may be observed that a' - values need to be quite large for high values of λ_{\min} . Indeed, it may be noticed from figure 17, that the grating no. 10 with a' - value of 776nm provides perhaps as good a spectral response as can be expected using a single sinusoidal phase grating. however, its transmittance in the

wavelength range of the visible spectrum is quite small and a transmittance of 10-15% in wavelength range of 800-1000nm may also be unacceptably hazardous. These results thus show the limitations of the applications of single sinusoidal gratings to restrict the transmittance of harmful coherent radiations in a satisfactory manner, although over a narrow range of wavelength the sinusoidal gratings with appropriate groove depths would be a satisfactory and relatively inexpensive method for a protection against harmful radiation.

4.2 Groove Depth Determination by SEM Technique

The NPL were unable to provide information on the groove depths (a' - values). An attempt was made in our laboratories to measure the physical peak to peak amplitude with a Scanning Electron Microscope (SEM) using a shadow graph technique in which the electron beam of the SEM was incident on a grating surface at an angle of 15° . The shadow cast by the groove was then measured and the groove depth calculated. A typical SEM result of groove shadow casting is shown in figure 19 for the Grating no. 10 and the calculated groove depth from it appears to be $\sim 830\text{nm}$ which is within 7% of the estimated value of a' using the equation 7. It may thus be argued that equation 7 provides a reasonable estimate of the sinusoidal grating physical groove depth from an experimental determination of the λ_{\min} value at which the transmittance is minimum.

4.3 Crossed Gratings On Different Substrates (NPL)

The transmittance through two superimposed grating system is the product of the two individual grating transmittances. For two crossed sinusoidal gratings of optical peak to peak amplitude a_1 and a_2 the transmittance is given by [2],

$$T(\lambda) = J_0^2 \left(\pi a_1 / \lambda \right) J_0^2 \left(\pi a_2 / \lambda \right) \dots (8)$$

where $T(\lambda)$ is the transmittance, (i.e., zero order efficiency) and J_0 the Bessel function of zero order and first kind.

A crossed two grating system was investigated experimentally using (gratings Nos. 1 and 10 with a' - values of 637nm and 776nm) with their corrugations crossed, i.e., mutually perpendicular), these two groove depths being the shallowest and the deepest respectively amongst the ten gratings provided by the NPL. The spectral response of this system is shown figure 20 from which it may be seen that the region of minimum transmittance has been extended in the wavelength range of 500nm to 1000nm with maximum transmittance not exceeding 6% at the two extreme ends. Thus although such a crossed grating system is quite effective in providing a wide and extremely low transmittance band, the visibility through the crossed grating system at optical frequencies remains very low.

4.4 Crossed Grating System On A Single Substrate (NPL)

The effects of the spectral cut off bandwidth with two crossed grating system may be achieved using a single two-dimensional phase grating (see figure 5) on one substrate. Two such photoresist and crossed gratings of

unspecified groove depth values were provided (Gratings Nos. 11 and 12) by the NPL.

A preliminary examination of these two gratings (Nos. 11 and 12) showed that the optical plane of one or both axes on each grating was not coplaner with the substrate. Both gratings were found to have a first order diffraction angle β_1 , of 22° in both cases, thus giving a grating period d , of $1.67\mu\text{m}$ or 600 lines per mm. The angle of doubly diffracted β_{11} beam was found to be 30° , as expected. The transmission spectrum for the Grating No. 11 is shown in figure 21 from which it may be seen that λ_{min} is at 750nm (0.5% transmission), thus giving a profile depth a' - value of 896nm and an optical amplitude a - value of 573 nm. It may also be observed from figure 21 that the zeroth order transmittance does not exceed 10% in the wavelength range 450nm to 1000nm. The transmittance spectrum and the groove depth of the second NPL crossed grating (no. 12) were observed to be similar to that of the Grating No. 11. Both the crossed gratings show promise to meet our preliminary requirement although the transmittance (%) in the visible region of the spectrum remains again very low.

4.5 Optometrics Single Sinusoidal Gratings

The two identical gratings (Nos. 13 and 14) provided by the Optometrics (U.K.) Ltd are commercially available products with unspecified groove depth. Figure 22 shows the transmittance spectrum of Grating 13 which has a λ_{min} at 450nm (6% transmittance). This indicates a physical groove depth (a') of 537nm. Both the gratings (Nos. 13 and 14) have 600 lines per mm ($d = 1.67\mu\text{m}$). However, Grating No. 13 exhibited a lower transmittance than the Grating 14 which suggests that the former grating has a better sinusoidal profile, the result being closer to the theoretical case), than that of the latter grating. It became obvious that the two gratings provided by the Optometrics (U.K.) Ltd., could not produce the required rejection band because of their too shallow groove depth (a'). The manufacturers were unable to provide us with gratings possessing deeper groove depths.

Note: All fourteen gratings (twelve from NPL and two from Optometrics) were handed over to Dr. R.J. Shuford at the end of their transmittance study in our laboratories.

The results given above, indicate that it is possible to obtain a high degree of attenuation in the zero order beam for a small rejection band of wavelength using a sinusoidal photoresist phase transmission grating of appropriate values of the period (d - value) and the groove depth (a' - value).

The greater the groove depth is, the larger is the value of λ_{min} at which the transmittance of the coherent radiation is minimum. However, it becomes quite difficult to produce very deep groove depth on a photoresist by the holographic technique with good sinusoidal pattern and repeatability. Although both NPL and Optometrics were unwilling to provide a measure of the groove depths of their gratings, it appears that the technique of shadow casting, used in this work with a Scanning Electron Microscope in which the grating plane is held at a suitable tilt

angle to the electron beam, provides a measure of the groove depth which is in reasonable agreement with the estimated value from the location of λ_{min} in the transmittance spectrum.

If the amplitude of the profiles are dissimilar, the range of wavelengths over which the incoming beam is attenuated is increased. By a suitable choice of two dissimilar groove amplitudes with two separate crossed gratings or crossed groove profiles on a single glass substrate a wide rejection band in the spectral range of ~ 500 to 1000nm may be obtained.

These results satisfy the specification which was required of us to fulfill. It should, however, be noted that the transmittance in the visible part of the spectrum is quite low for a crossed sinusoidal grating and thus unsatisfactory.

It was then requested in May 1991 that we should consider a change in specification such that the fast acting optical system should have ~ 50% transmission at 650nm (i.e. a good transmittance in the visible frequency region of the spectrum) and that the transmittance should be as little as possible in the wavelength region 650nm, extending up to, say, 1000nm. These new requirements are substantially different from the earlier objectives which was to obtain a maximum attenuation in the widest possible region of the visible spectrum.

Now the extent of the development and applications of dielectric thin films in optics as edge filters are well documented. In optical edge filters metallic and dielectric thin films are combined in a multilayer system. In devices, consisting of all dielectric layers, designed for use in the visible region of the spectrum, the layers usually consist of magnesium fluoride and zinc sulphide.

5 Principles of Multilayer Dielectric Thin Film Mirrors (i.e. Filters)

The principle, governing the operation of a dielectric thin film mirror, is in the interference of radiation waves in a multilayer system in which there should be very little absorption. The determination of the fraction of the incident electromagnetic radiation transmitted or reflected from a dielectric film, requires solving a second-order differential equation which satisfies the boundary conditions, i.e., that the components of the electric and magnetic fields tangential to the boundaries of the film be continuous across the boundaries. The theoretical analysis of the process is adequately described by Lissberger⁵ and will not be given here.

The design of dielectric mirrors can be deduced from the well known generalized Airy formula which allows to calculate the transmittance and reflectance of a multilayer system as a function of frequency. The simplest mirror system consists of a number of dielectric layers with alternating high (H) and low (L) refractive index, each being a quarter wave in optical thickness at the design wavelength (figure 23). The reflectance R, of such a mirror system is given by,

$$R = \left[\frac{1 - \eta}{1 + \eta} \right]^2 \quad \dots (9)$$

$$\text{where } \eta = \frac{n_2}{n_0} \left[\frac{n_1}{n_2} \right]^{2N} \text{ or } \frac{n_1^{2N+2}}{n_0 n_2^{2N}} \quad \dots (10)$$

for $2N$ or $2N + 1$ layers respectively. Here n_s is the refractive index of the substrate, n_1 and n_2 are the low and high refractive indices of the alternate dielectric layers respectively and n_0 the refractive index of air ($n_0 = 1$). At wavelengths sufficiently removed from the design wavelength λ_0 , the reflectance of the system would fall as the phase relationship between the reflected beams which favour a high reflectance will be disturbed. However, if the number of layers in the system is large the width of the wavelength range over which the reflectance remains high, can be extended. Figure 24 shows the computed spectral reflectance of periodic quarter-wave reflector of zinc sulphide ($n_2 = 2.35$) and magnesium fluoride ($n_1 = 1.38$), deposited on glass ($n_s = 1.52$) for different number of layers⁵.

Such multilayer dielectric mirror systems can be used as the basis for the design of edge filters which have sharp transitions between the pass band and stop band in their spectral transmittance curves, since $T = 1 - R$ for all dielectric systems where T and R are the transmittance and reflectance respectively. The sharpness of the transition improves as the number of layers is increased, although both the amplitude and the frequency of oscillations increase unfortunately at the same time. However, these ripples can be reduced by matching properly the values of the high and low refractive indices. Dielectric mirrors are usually designed for operation at normal incidence of the radiation. For applications with a wide range of angles of incidence, the performance of the mirror deteriorates although it is now possible to minimize this effect by using materials with high refractive indices. The major difficulty lies in obtaining a uniform deposition of layers over the desired area of the filter. The theory and practice of vacuum deposited layers on a rotating substrate is now well established and the characteristics of the vapour source are also reproducible. For reasonable deposition rates, the vapour pressure in the vicinity of the source is usually of the order of one torr and the extent of the vapour cloud in this region is governed by the temperature of this source which affects the spatial distribution of the molecules and hence the thickness distribution of the film condensed on the substrate. The reproducibility of the thickness distribution requires a good control of all the factors which affect the scattering of vapour molecules. The limitations of these mirrors (or edge filters) is the scattering due to inhomogeneities and surface roughness of the layers which are attributable to the particulate nature of the dielectric materials.

To ensure that the finished product has the desired optical properties, the coating process has to be organized so that the basic optical parameters of the individual layers, i.e. the refractive index and the film thickness conform to the design specifications within appropriate limits. The refractive index of a thin dielectric film for a particular dielectric material will depend on the rate of evaporation, substrate surface structure, temperature and residual gas composition which are difficult to bring under close control. As regards optical thickness, there is a major practical problem, i.e. precise control of the layer

thickness during deposition. The transmittance of the coated surface goes through a maximum or minimum value at the design wavelength λ_0 whenever the optical thickness of the film reaches a multiple of $\lambda_0/4$. A monochromatic beam of radiation at a wavelength of λ_0 of constant intensity is directed at the substrate surface and the intensity of the reflected or transmitted beam examined by a suitable linear detector. The deposition of a particular layer is terminated when the detector output reaches the appropriate level. In practice, the monitoring system is much more sophisticated in which the reflectance and the transmittance of the coating is differentiated with respect to wavelength and when the first derivative is zero, a deposition reaches its end point. The present practice is to maintain the substrate at ordinary temperatures during the deposition process.

5.1 Results & Discussions: Dielectric Mirrors

PL Coatings Ltd. of Belfast, Northern Ireland, undertook to provide us with two dielectric mirrors on a 50mm diameter glass substrate with the following specifications:

"Transmittance greater than 0.8 from 0.4 μ m to 0.62 μ m and reflectance greater than 0.8 from 0.67 μ m to 1.06 μ m".

Both surfaces of the glass substrate were employed by the manufacturer to produce these mirrors. Figures 25 and 26 show the spectral behaviour of these two dielectric mirrors, the characteristics being obtained in our laboratory using an optical densitometer which was designed and constructed by us. These results shown in figure 25 indicate that at normal incidence the transmittance is virtually unchanged in the stopband and that in the passband it is less by about 4% from the calculated value which corresponds to the reflectance of the uncoated substrate surface. At 60 degrees incidence for P- polarised radiation, the transmittance is again very little changed over the entire spectrum because this is close to the Brewster angle (56.7 degrees) for the substrate material. For the S- polarized radiation at 60 degree incidence, the transmittance in the passband is reduced by 25% because the reflectance of the uncoated substrate surface is enhanced under these conditions.

Both the surfaces of the glass substrate for the second dielectric mirror were coated identically before the deposition of the films. The spectral response (figure 26) with such treatment shows that the stopband edges become much sharper but the ripples in the passband become larger, unfortunately.

Following this progress, a dielectric mirror of twenty four layers with alternate zinc sulphide and calcium fluoride dielectric layer on a polycarbonate of substrate was produced by PL Coating Ltd. to satisfy the following desired criteria:

- (i) $T(av) > 0.5$ for $410\text{nm} < \lambda < 500\text{nm}$ and $560\text{nm} < \lambda < 640\text{nm}$
and
- (ii) $T < 0.05$ for $680\text{nm} < \lambda < 1110\text{nm}$.

Two dielectric mirrors were fabricated on separate polycarbonate

substrates which were attached face to face with UV cured glue along the substrate edges. Two such devices, termed PLC1 and PLC2 were tested in our laboratory and figure 27 shows the behaviour of the normalised transmittance of both at normal incidence in the spectral range specified above. It may be observed that the spectral response (figure 27) is in good agreement with the desired specification at wavelengths $>650\text{nm}$ and at 532nm which are the two important areas in requirement for laser protection. The reason for the observed difference in the transmittance at wavelengths $<500\text{nm}$ between the two mirrors PLC1 and 2 is not obvious. Although the visibility through the dielectric mirrors and the spectral response are well acceptable, a deterioration of the dielectric surface was observed which has been attributed to the UV curing of the glue and this needs to be avoided.

Figure 28 shows the normalized transmittance of PLC1 dielectric mirror for varying angles of incidence from 0° (normal incidence) to 60° in the spectral range of $400 - 1000\text{nm}$. It may be noticed that a progressive departure from the normal incidence decreases the transmittance and also the passband accordingly which are to be expected for the P-polarized light. For such cases, the term 'Beam Splitter' may be applied to a multilayer dielectric mirror system as an interaction of radiation with the multiple layers invariably leads to a splitting of the energy flow into the transmitted and reflected beams of complimentary intensities. As stated before, this effect can be reduced by increasing the number of layers of the dielectric films, but it cannot be eliminated as the impedance of the dielectric layer is different for the P- and S-polarization departing from the normal incidence.

Although the optical requirements were met satisfactorily with PLC1 and PLC2 dielectric mirrors, the innermost surfaces of the sandwich structure suffered deterioration due to UV curing of the glue, as stated above.

The next stage of progress was made when PL Coating Ltd produced a similar dielectric mirror of the sandwich structure, as described above, but no UV curing of glue was employed in this case. Figure 29 shows the characteristic transmittance spectrum of this sample for normal incidence.

It may be observed that the transmittance characteristics (figure 28) satisfy the required criteria although there are two considerable minor transmittance peaks ($\sim 3\%$) at 830nm and 970 respectively. In addition, there is also a broad shoulder of transmittance ($\sim 8\%$) at 690nm . The transmittance at 532nm was $\sim 3\%$ and the visibility through this dielectric mirror was good. No surface deterioration of the dielectric layers was observed with this sample.

At this stage, the MTL laboratory of the US Army, Watertown, MA asked for an even tighter specification in February 1992, which is as follows:

- (i) $<0.5\%T$ at 532nm
- (ii) $<1.0\%T$ at 694nm to 1064nm
- (iii) $50\%T$ (average) from 400nm to 500nm and from 560nm to 660nm .

The dielectric mirror should be formed by depositing appropriate layers on a single surface of one polycarbonate substrate with a uniformity of $\pm 1\%$ over 50mm diameter.

Above stringent requirements were met by the PL Coating and figure 30 shows the transmittance characteristics of this dielectric mirror which does not have the undesirable feature at 670nm which was present in previous mirror.

5.2 Conclusion

In conclusion, it may be said that the optical performance of the latest dielectric mirror satisfies the rigorous specification which is required for laser protection and the sophisticated technology is now available for fabrication of such mirrors at least for the substrate size of 50mm x 50mm x 3mm polycarbonate. However, such multilayer dielectric mirrors require further investigation for their stability of their optical properties under adverse conditions of temperature and atmospheric conditions under humid environment. Hard protective overcoating facility should also be explored for such devices.

References

1. L.P. Boivin,
Multiple Imaging Using Various Types of Simple Phase Gratings,
Applied Optics, 11, pp 1782-1792 (1972)
2. MT. Gale & K. Knop,
Surface Relief Images for Colour Production,
Focal Press (London, New York), chapter 2, pp 10-29 (1980)
3. M.T. Gale,
Surface Relief Gratings for Zero Order Reconstruction,
Optical communications, 18, pp 292-297 (1976)
4. H. Abramowitz & I.A. Stegun,
Handbook of Mathematical Functions, Dover (1988)
5. P.H. Lissberger,
Optical Applications of Dielectric Thin Films,
Rep. Progr. Phys., 33, pp 197-268(1970)
6. A. Thelen,
Design of Optical Interference Coating, McGraw-Hill (1990)

TABLE 1: Estimated values of physical groove depth a' , of NPL Sinusoidal Gratings.

Grating No.	λ_{\min} (nm) (experimentally determined)	$a' = 1.19 \lambda_{\min}$ (nm)
1	533	637
2	542	647
3	550	657
4	558	667
5	566	677
6	583	696
7	592	706
8	617	736
9	646	771
10	650	776

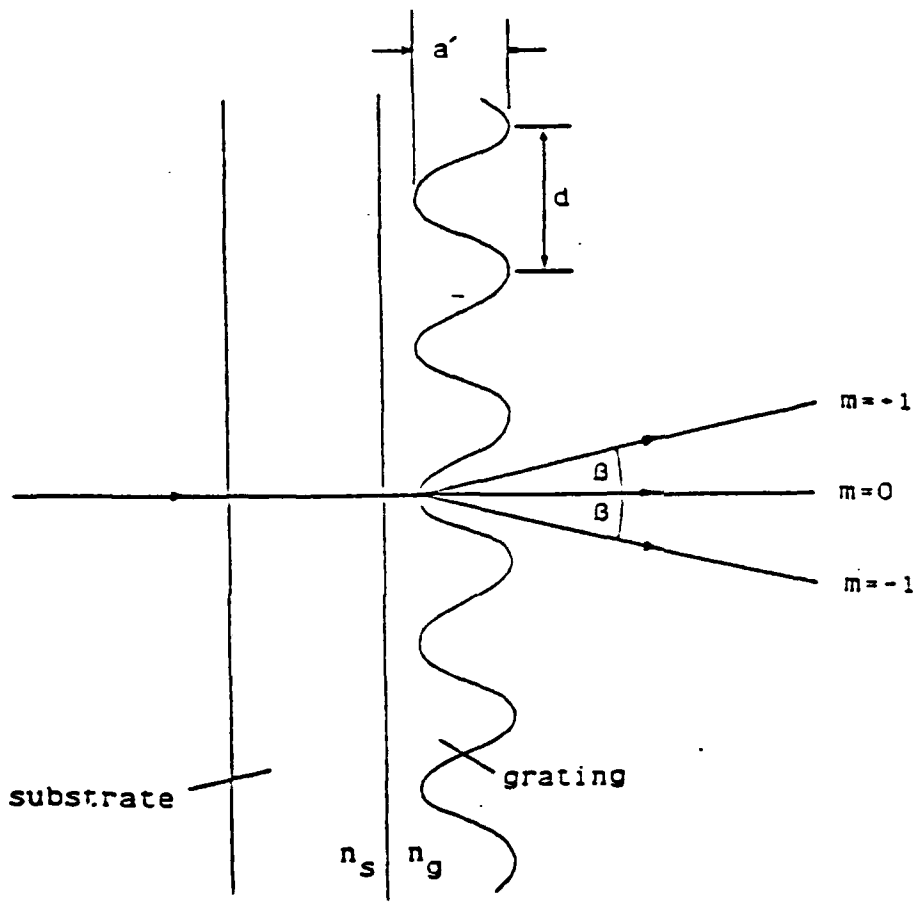


Figure 1. Sinusoidal Transmission Phase Grating

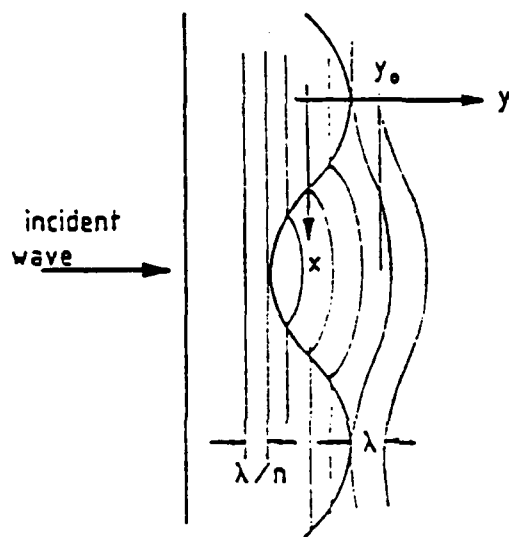


Figure 2. Distortion of plane wave due to grating profile.

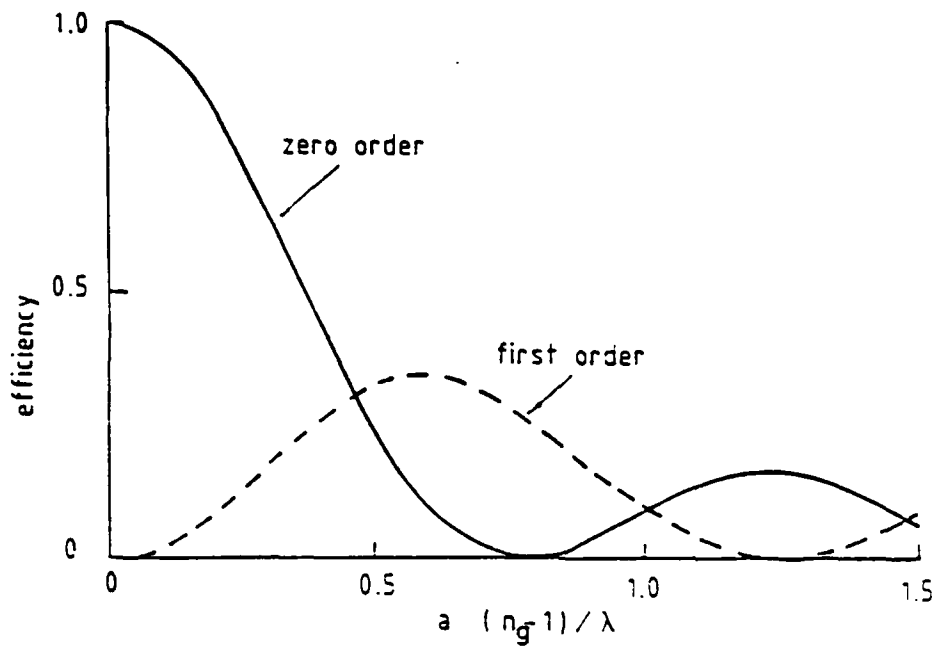


Figure 3. : Zero and first order diffraction efficiencies of a sine-wave phase grating (amplitude a , medium refractive index n_g) as calculated from Equation 4

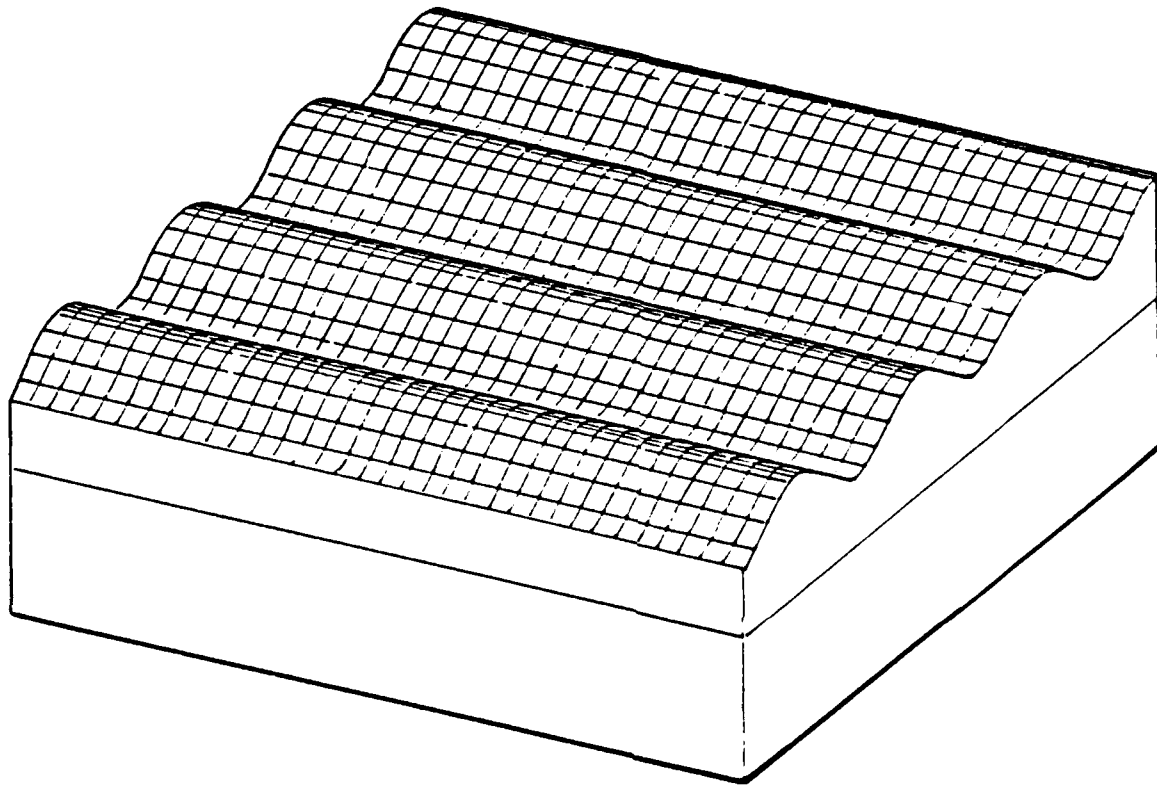


Figure 4. Section of a holographically produced , single profile, sinusoidal phase diffraction grating.

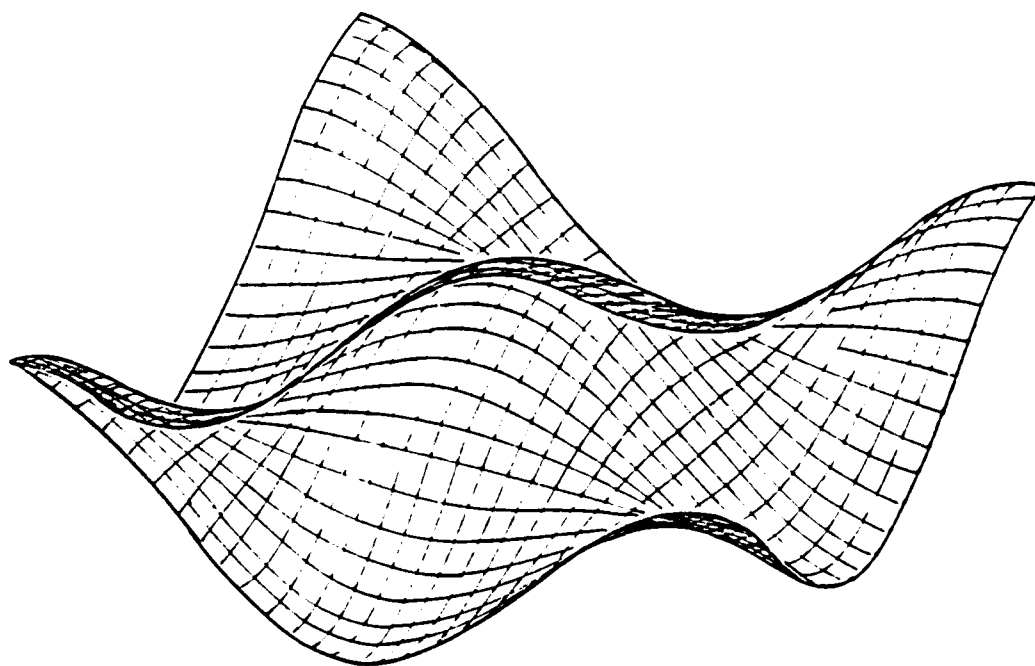
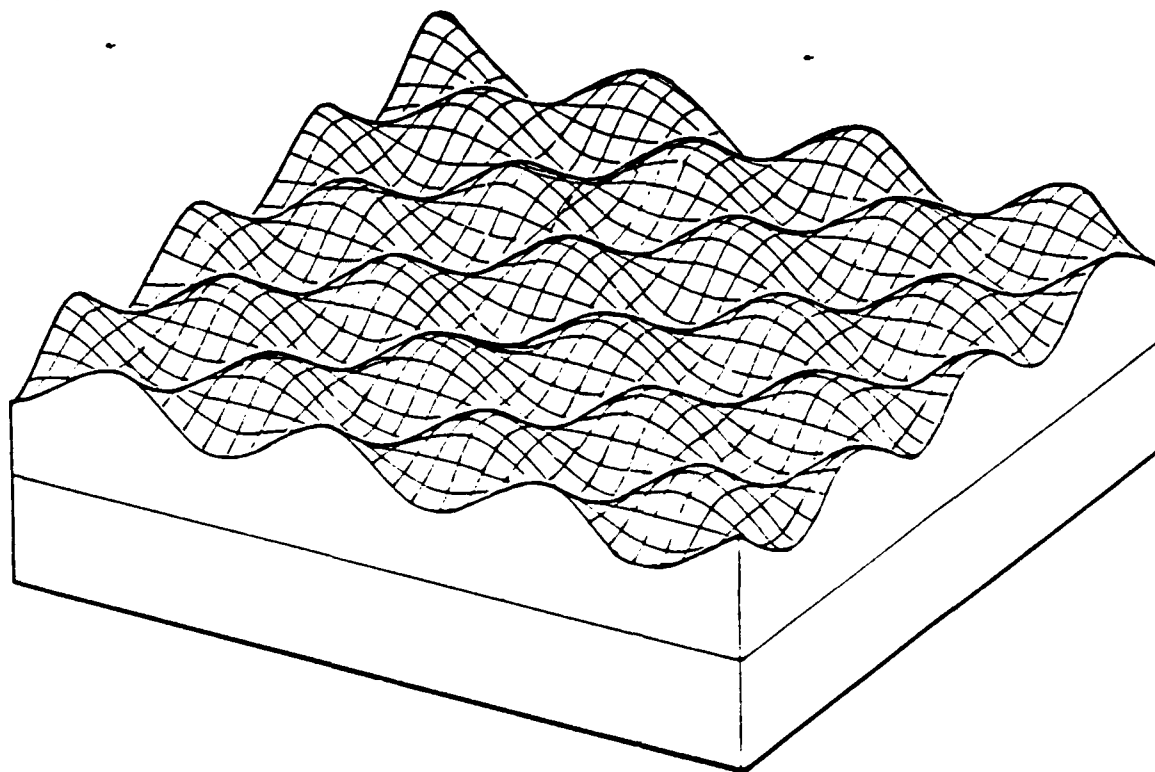


Figure 5. Two sections of a holographically produced, crossed profile, sinusoidal phase diffraction grating.

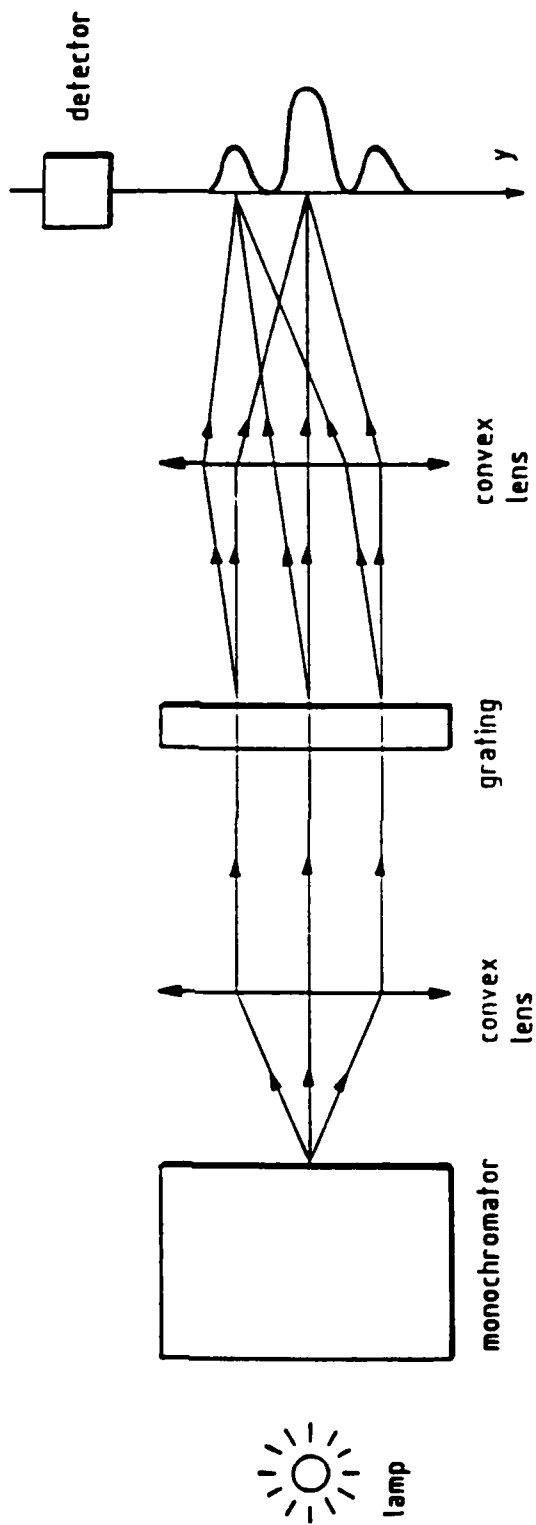


Figure 6. Wavelength response experimental arrangement .

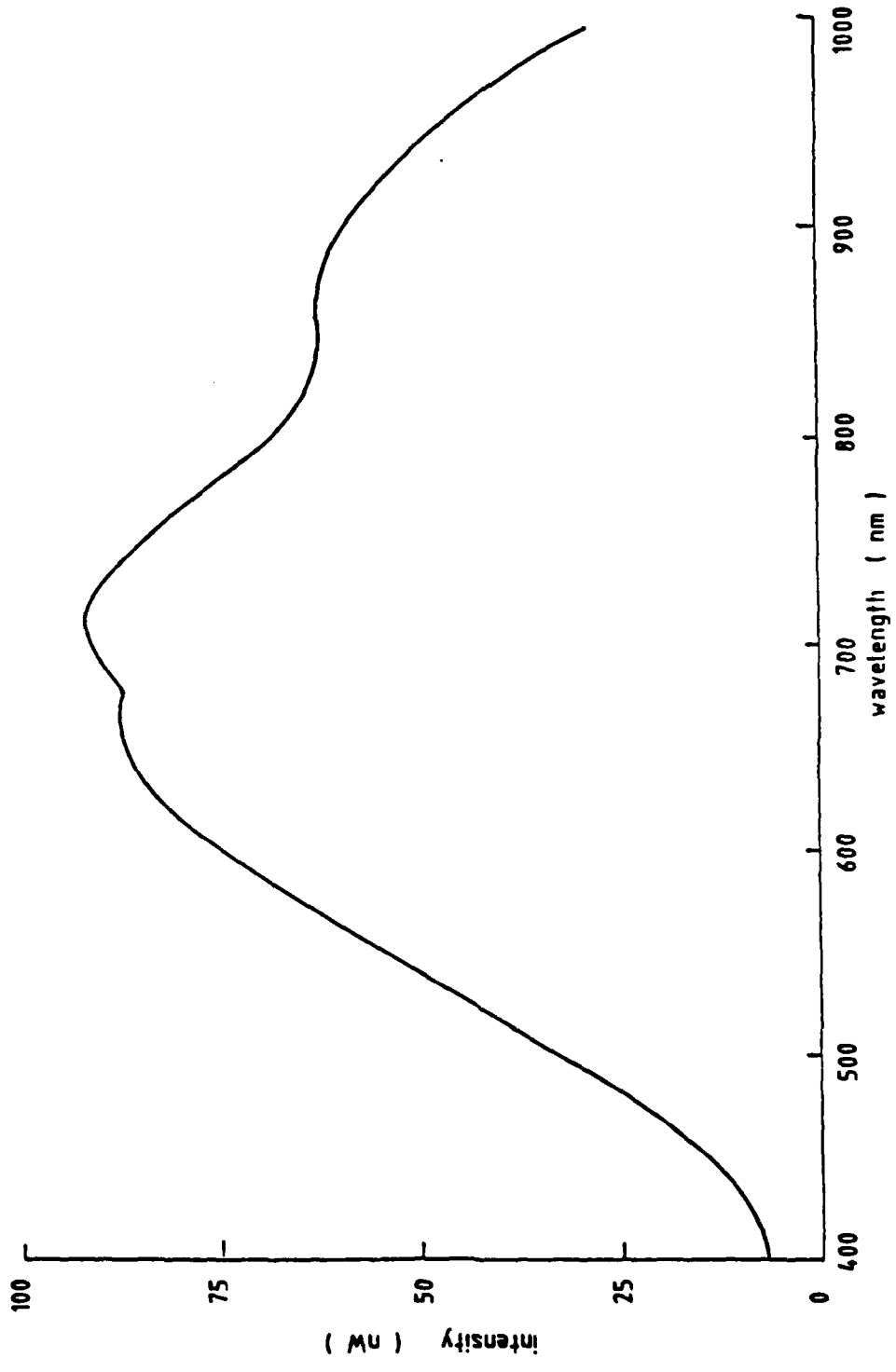


Figure 7 : Power spectrum of the light source.

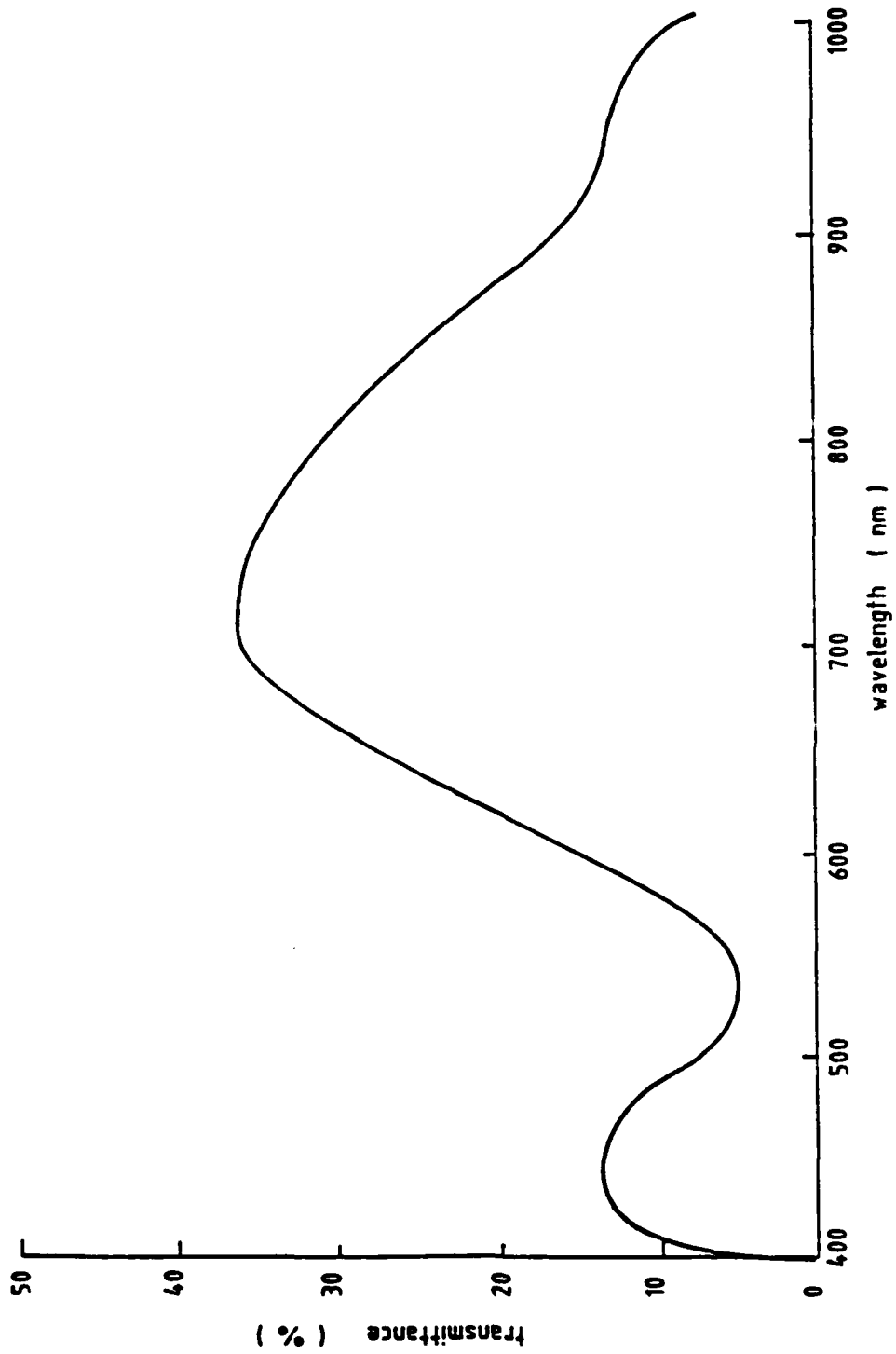


Figure 8. Normalized transmittance (%) / wavelength (nm) of grating 1 of groove depth 637 nm.

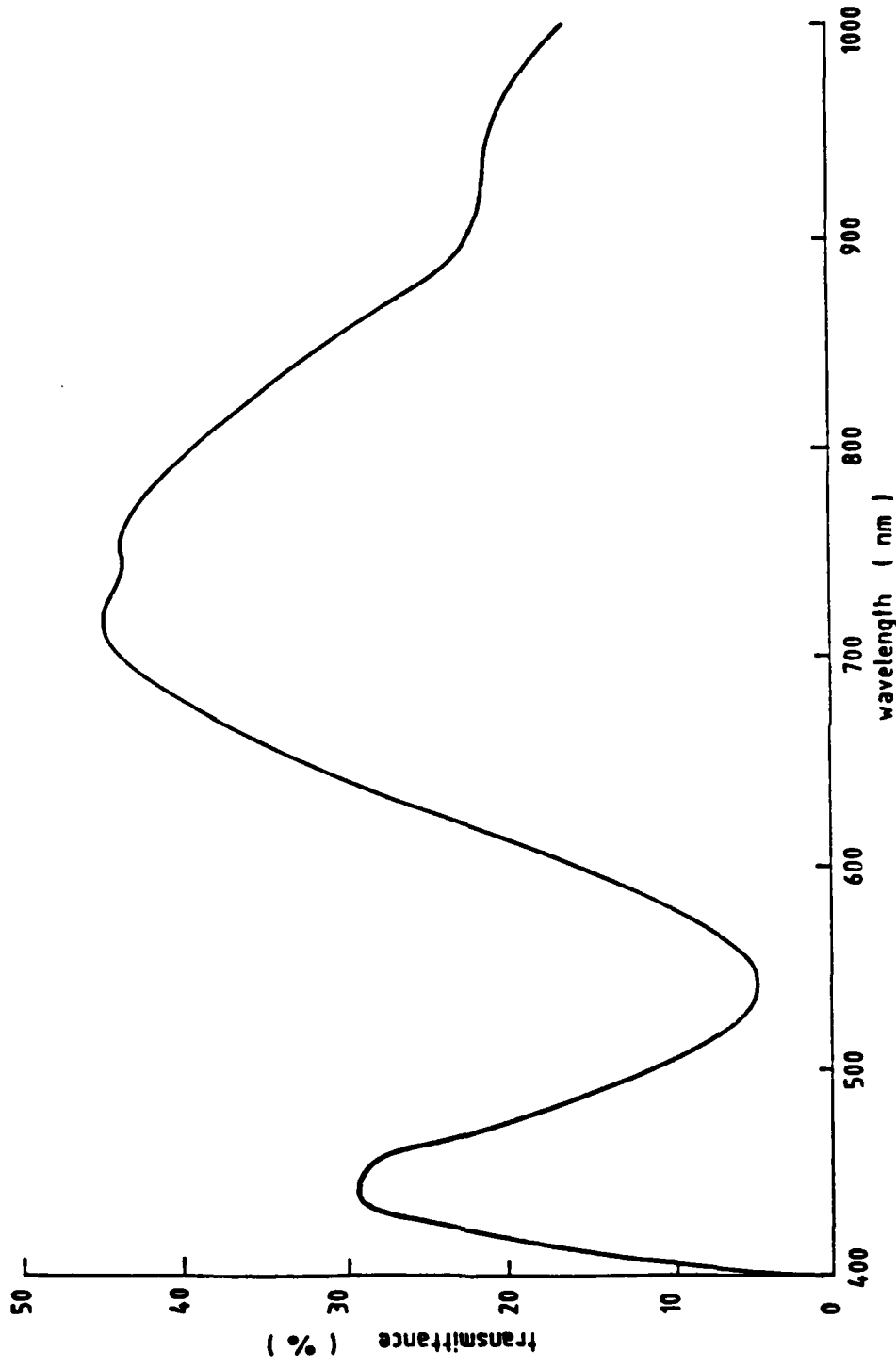


Figure 9. : Normalized transmittance (%) / wavelength (nm) of grating 2 of groove depth 647 nm .

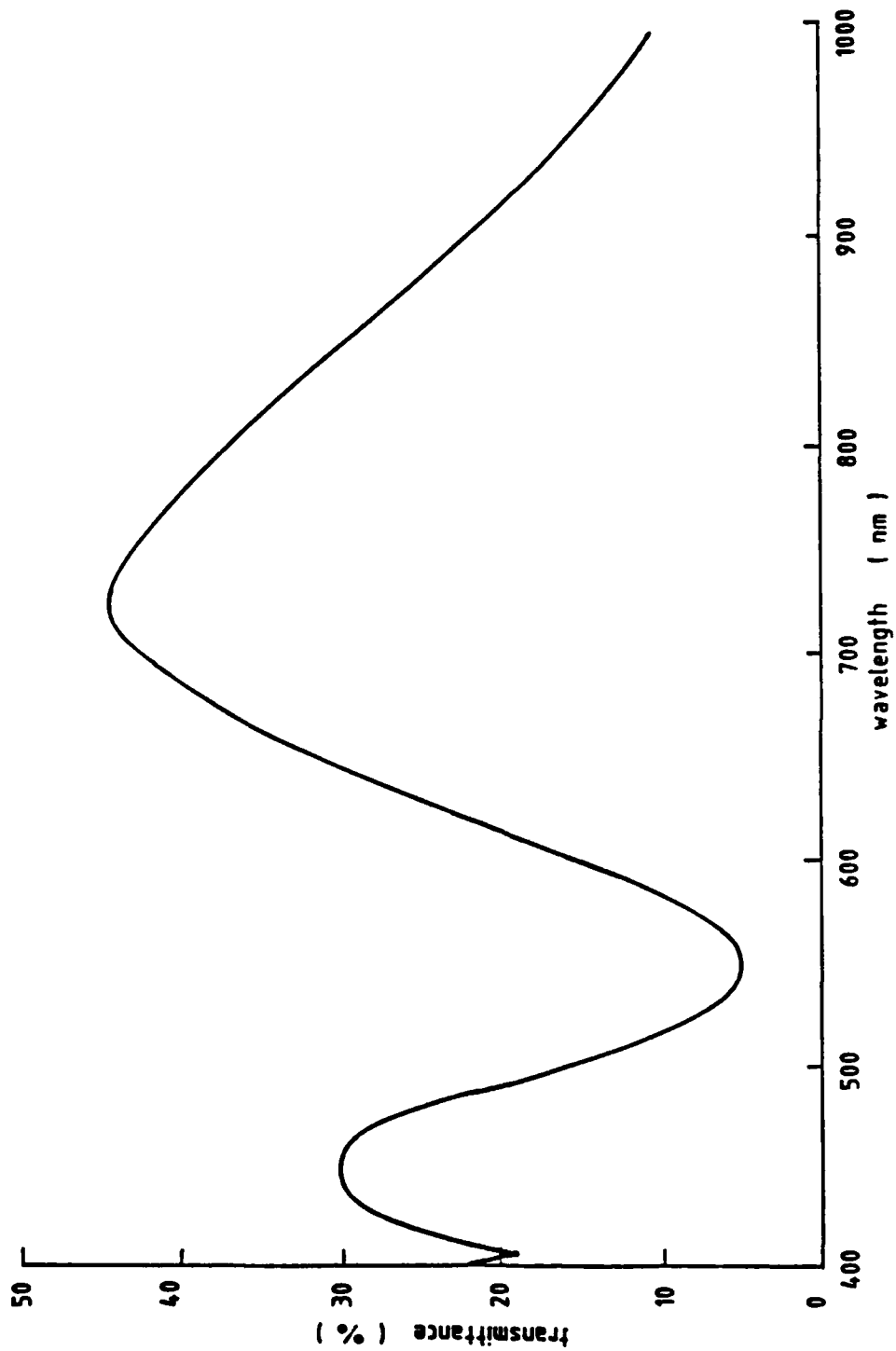


Figure 10. : Normalized transmittance (%) / wavelength (nm) of grating 3 of groove depth 657 nm .

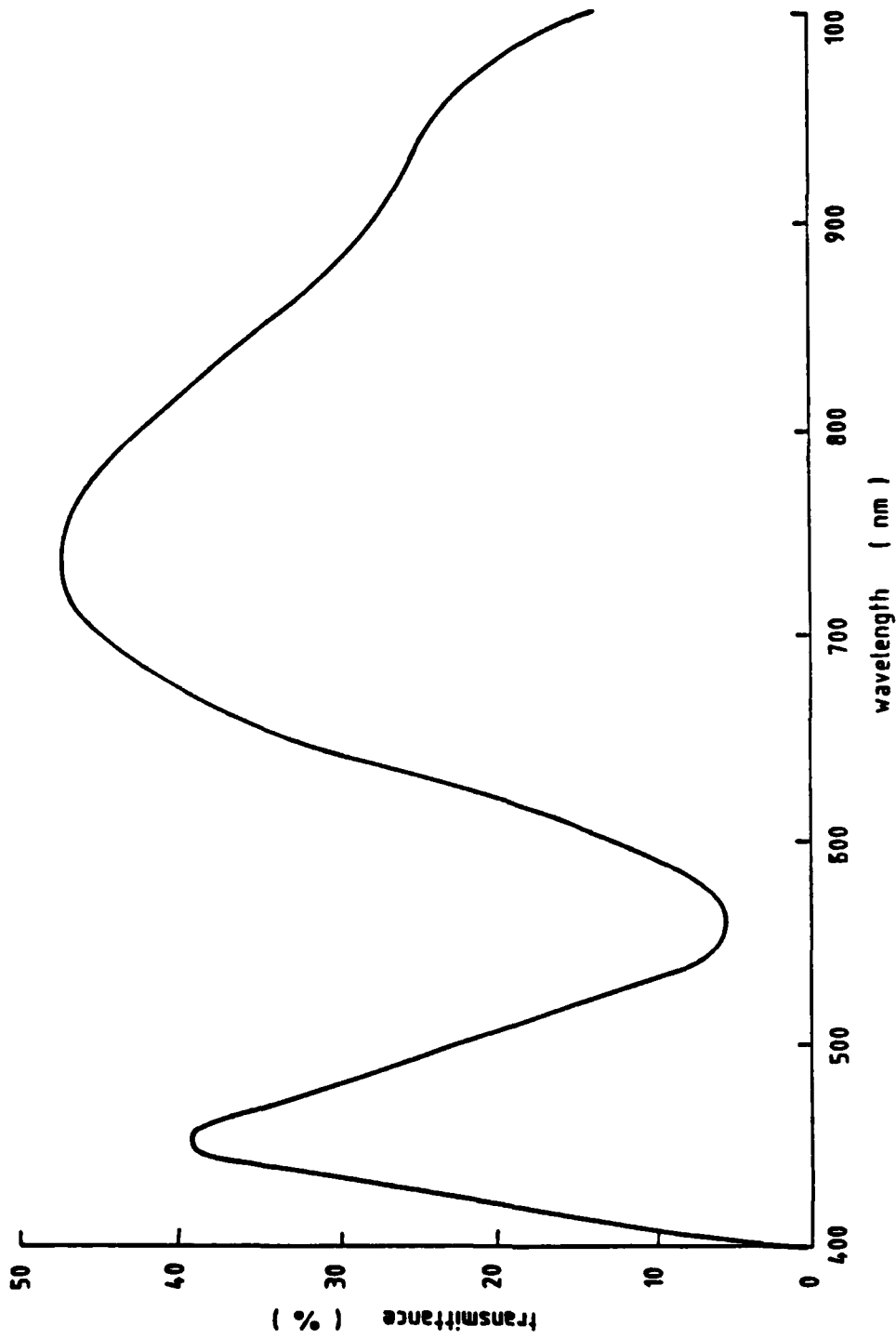


Figure 11. : Normalized transmittance (%) / wavelength (nm) of grating 4 of groove depth 667 nm.

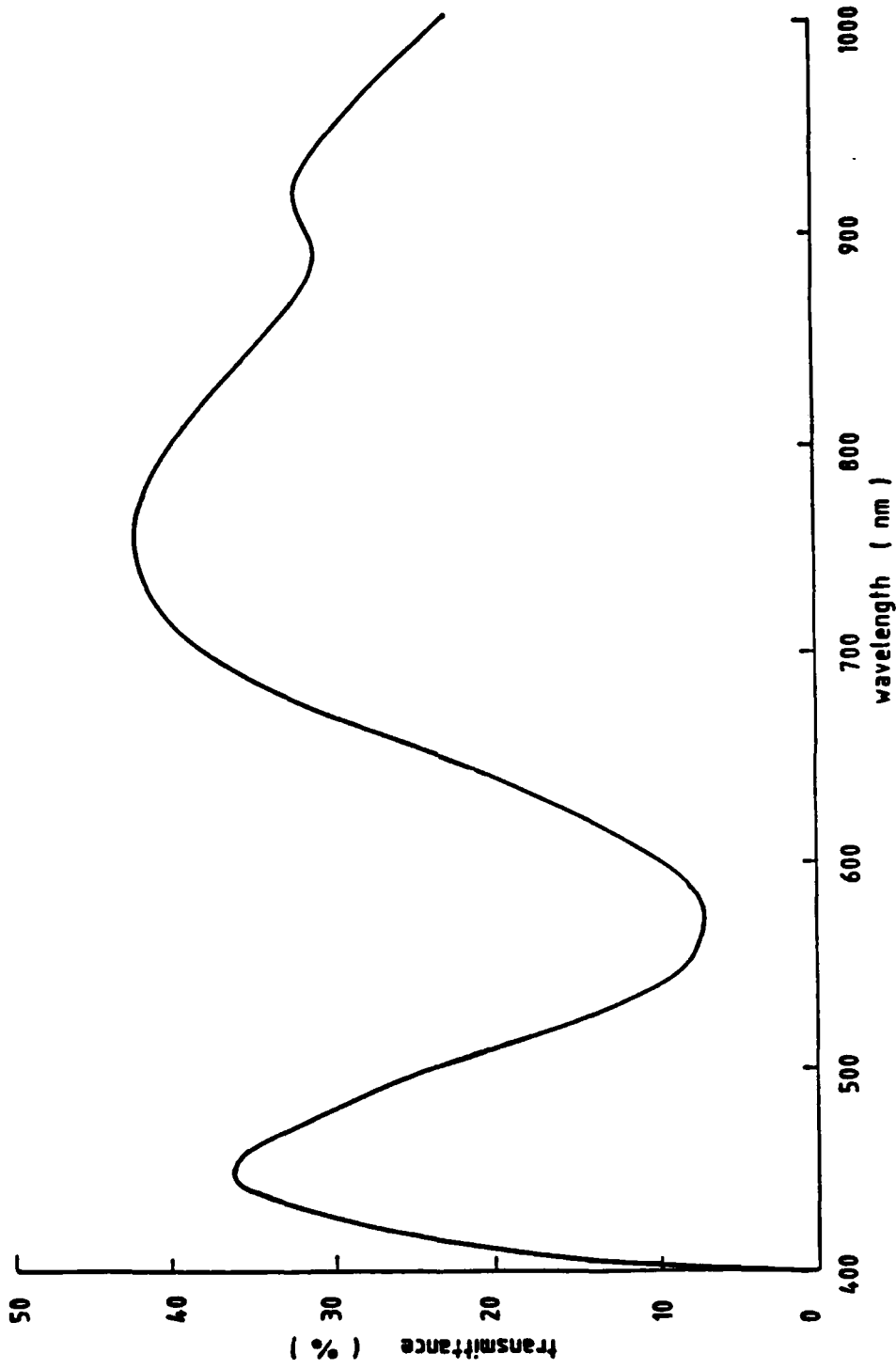


Figure 12. : Normalized transmittance (%) / wavelength (nm) of grating 5 of groove depth 677 nm.

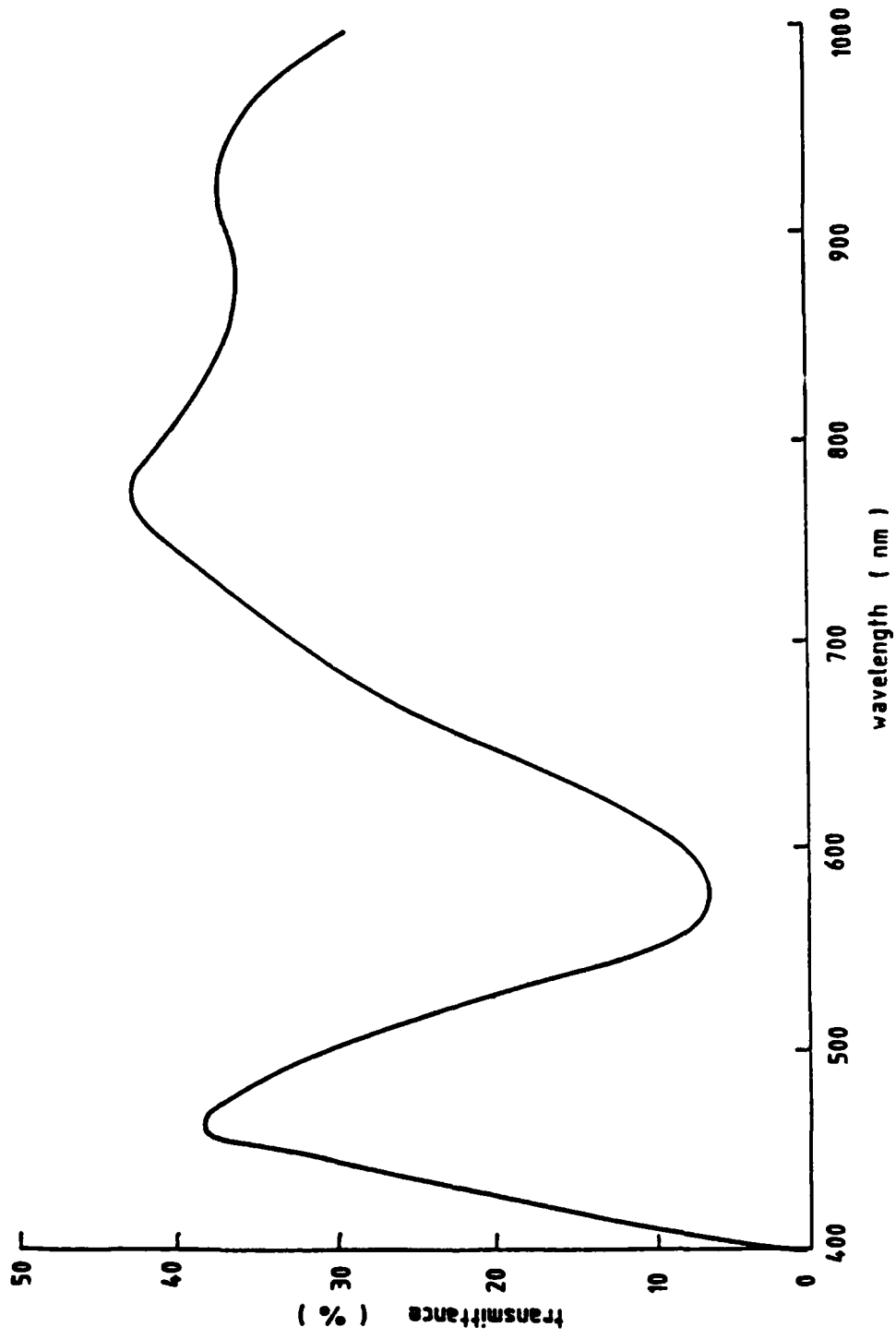


Figure 13. : Normalized transmittance (%) / wavelength (nm) of grating 6 of groove depth 696 nm .

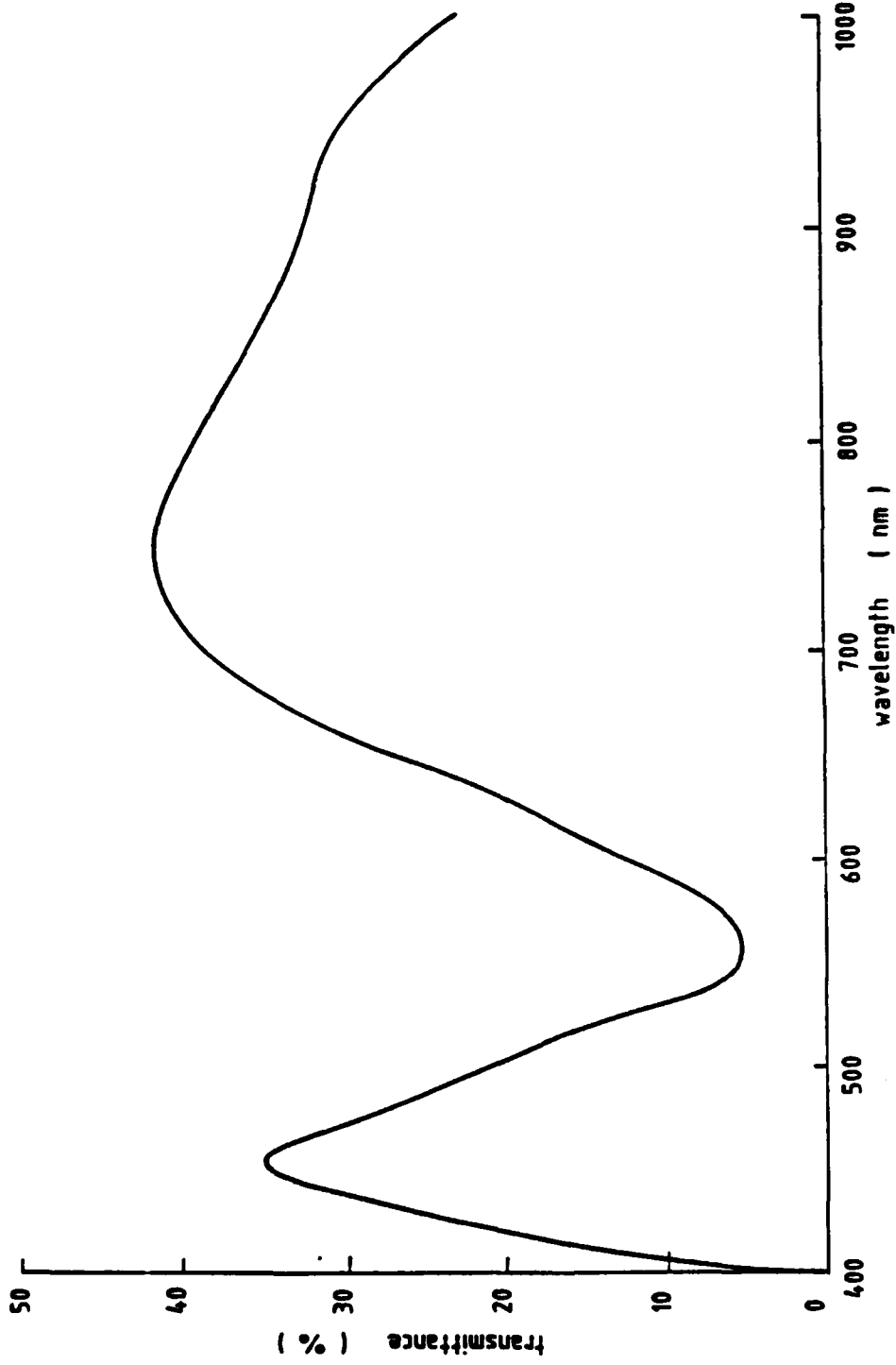


Figure 14. : Normalized transmittance (%) / wavelength (nm) of grating 7 of groove depth 706 nm.

1000

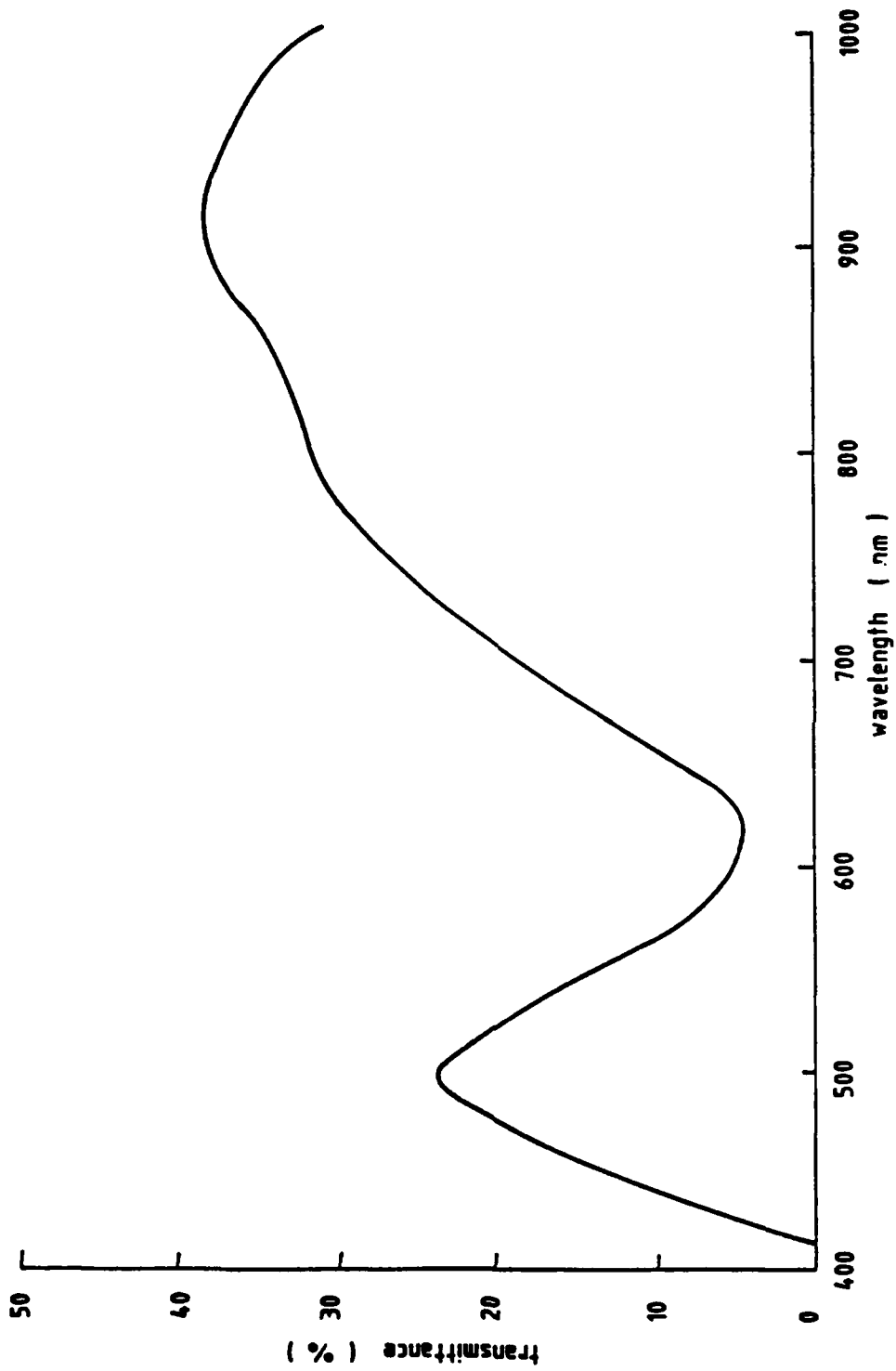


Figure 15. : Normalized transmittance (%) / wavelength (nm) of grating δ of groove depth 737 nm.

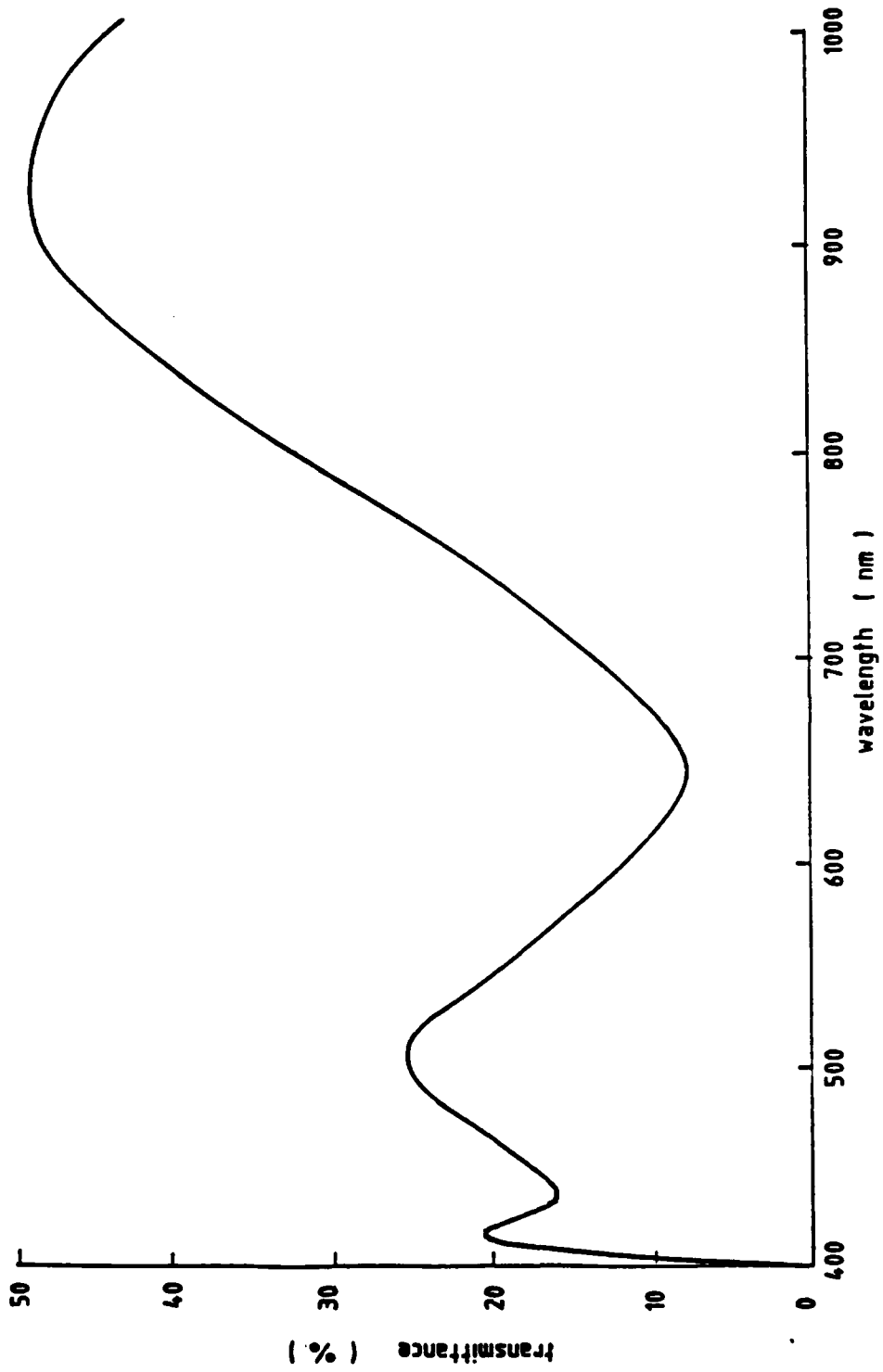


Figure 16. : Normalized transmittance (%) / wavelength (nm) of grating 9 of groove depth 771 nm.

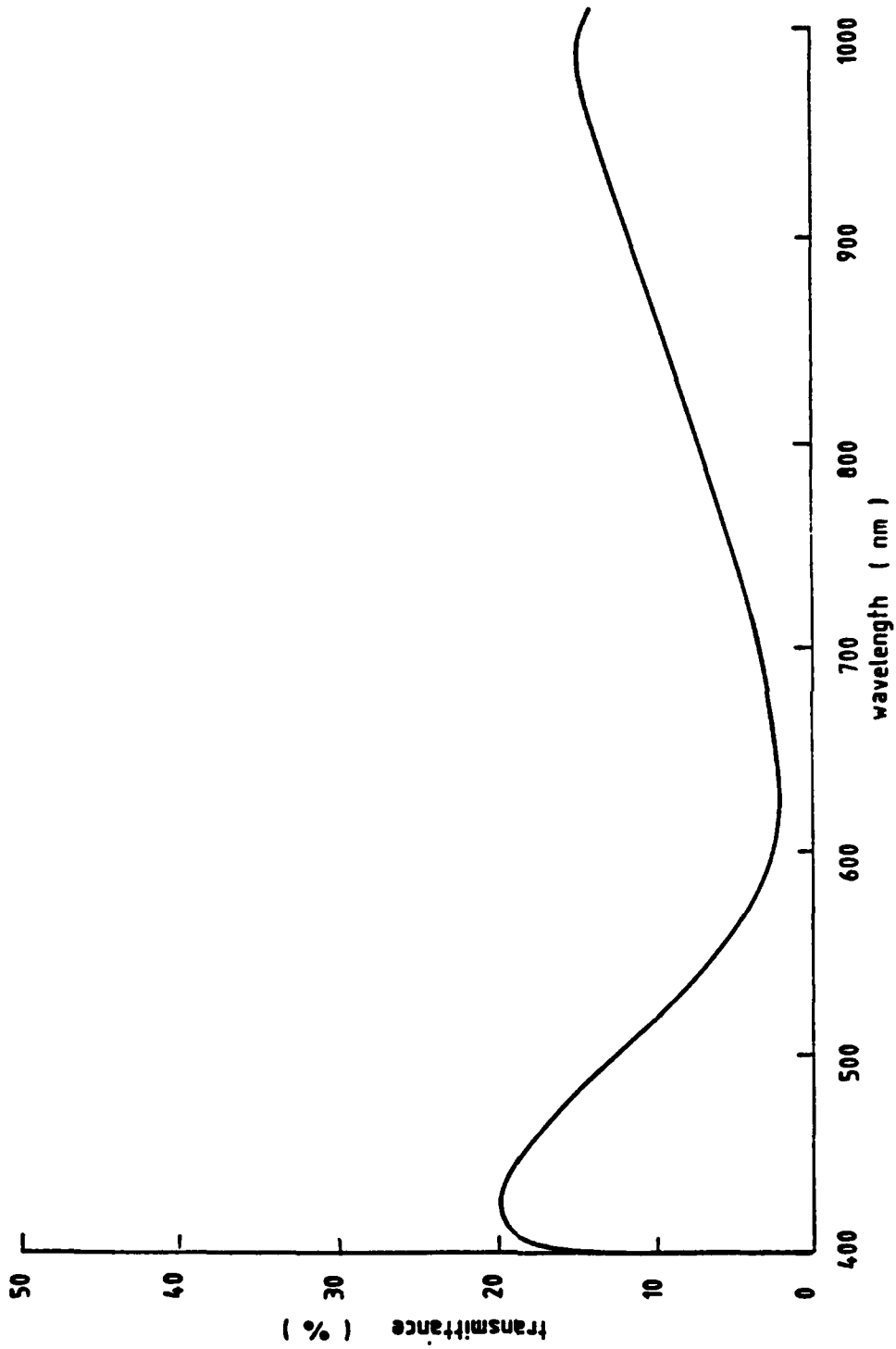


Figure 17. : Normalized transmittance (%) / wavelength (nm) of grating 10 of groove depth 776 nm .

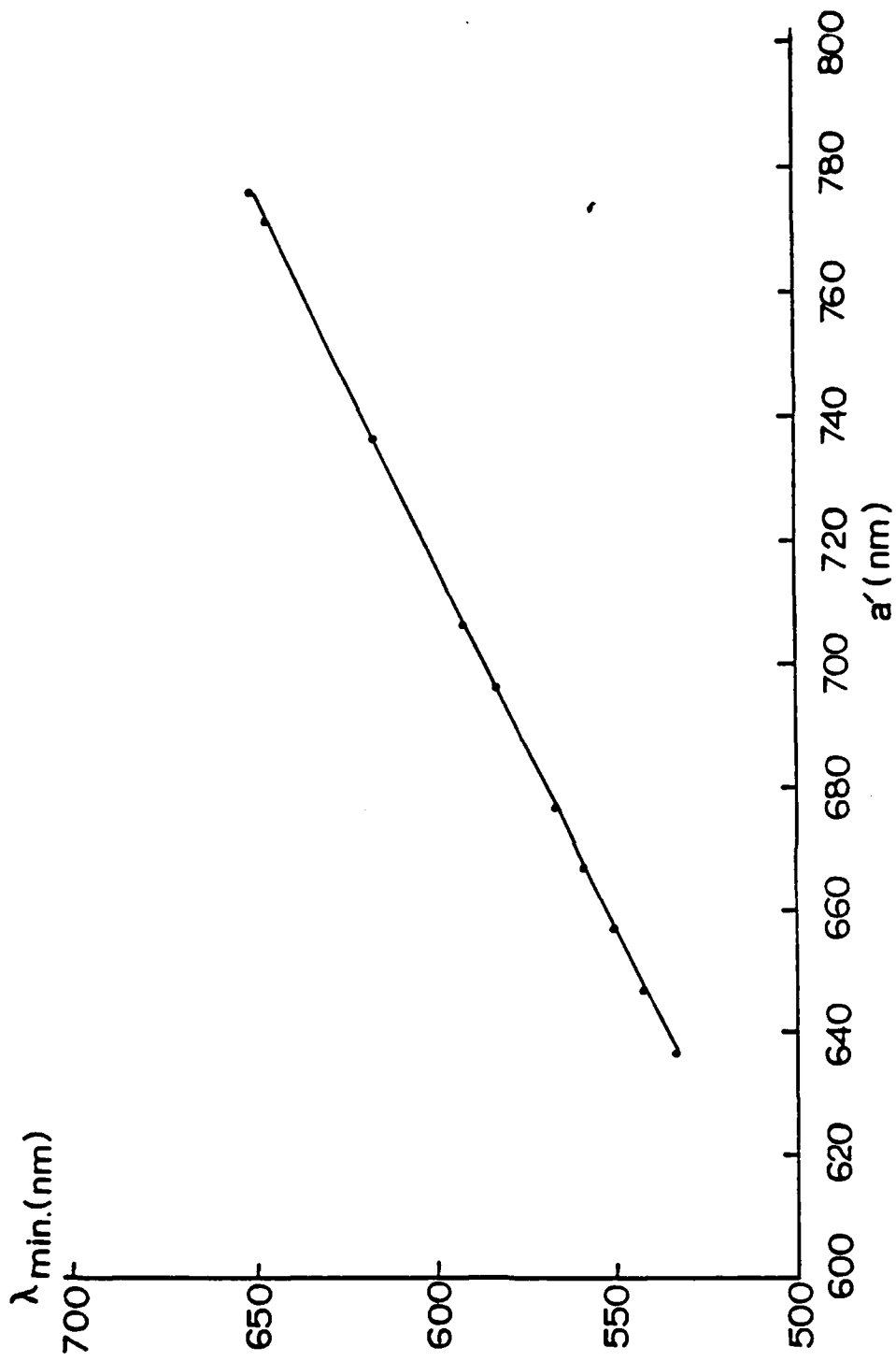


Fig 18. Behaviour of the physical groove depth a' and λ_{min} at which a minimum transmittance occurs.

Calculated groove depth = $a' = 830$ nm.
from the shadow cast. (cf. estimated from equation 7.
= 776nm.)

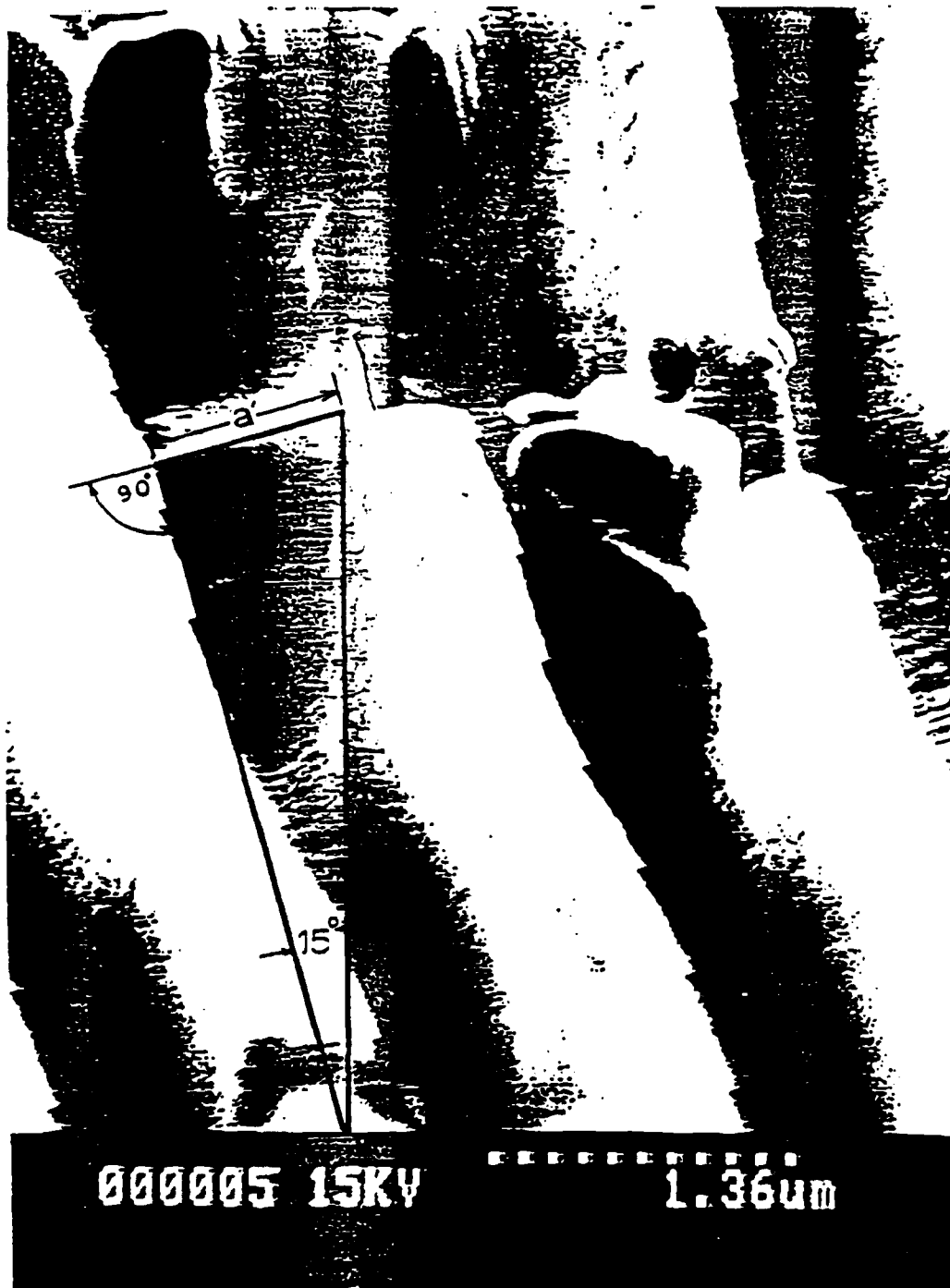


Fig.19. SEM Shadow casting in determining the groove depth of NPL grating 10.

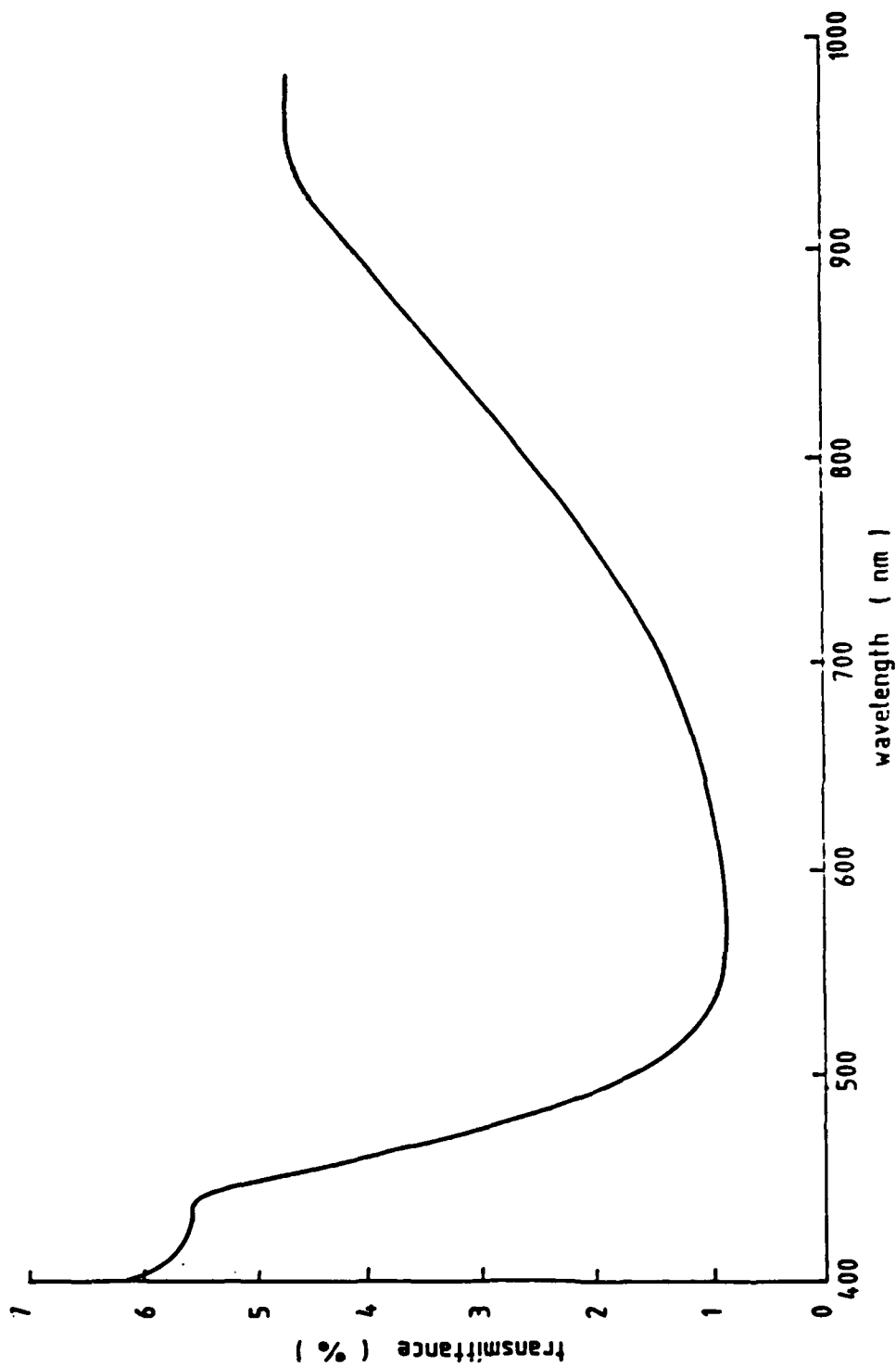


Figure 20.: Normalized transmittance (%) / wavelength (nm) for gratings 10 (776 nm groove depth) and 1 (637 nm groove depth) placed crosswise.



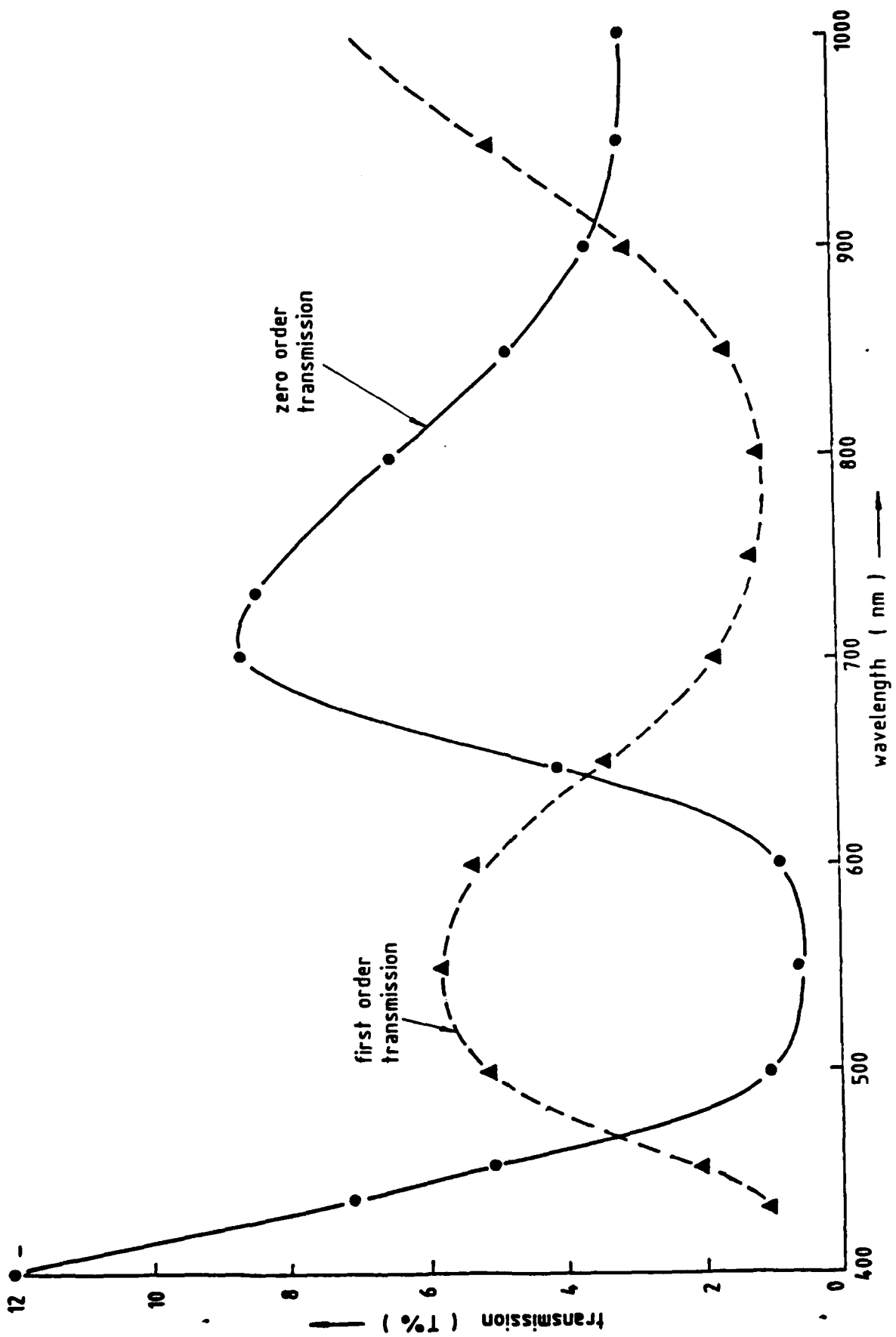


Figure 21.: Crossed sinusoidal photolith grating on glass substrate, 600 lines/mm, groove depth ~ 896 nm (estimated).

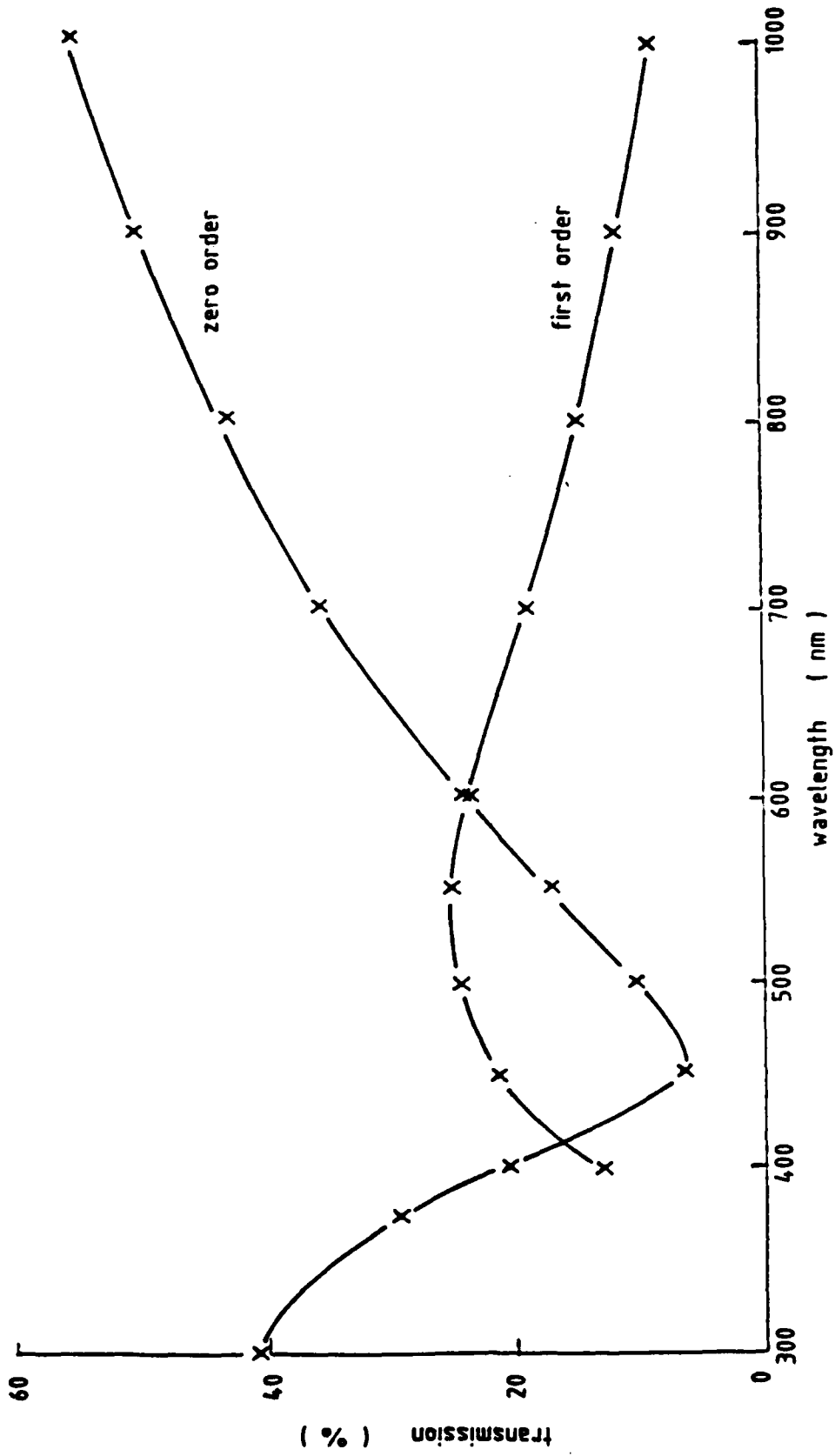


Figure 22. Normalized transmittance (%) / wavelength (nm) of grating 13 (Optometrics) of groove depth 537 nm.

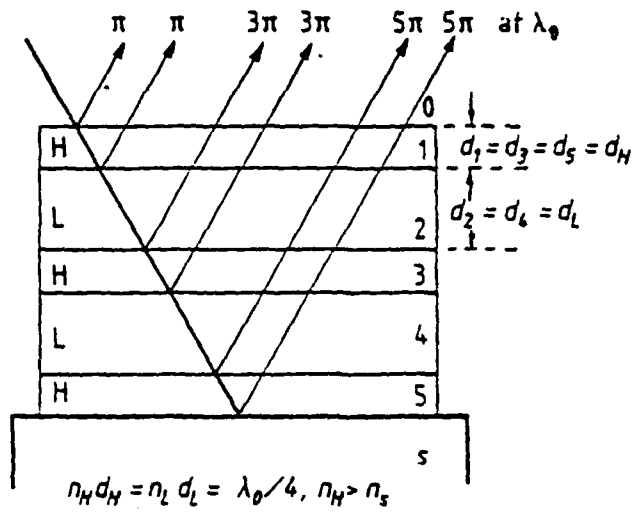


Figure 23 Simplified function of all-dielectric reflector.

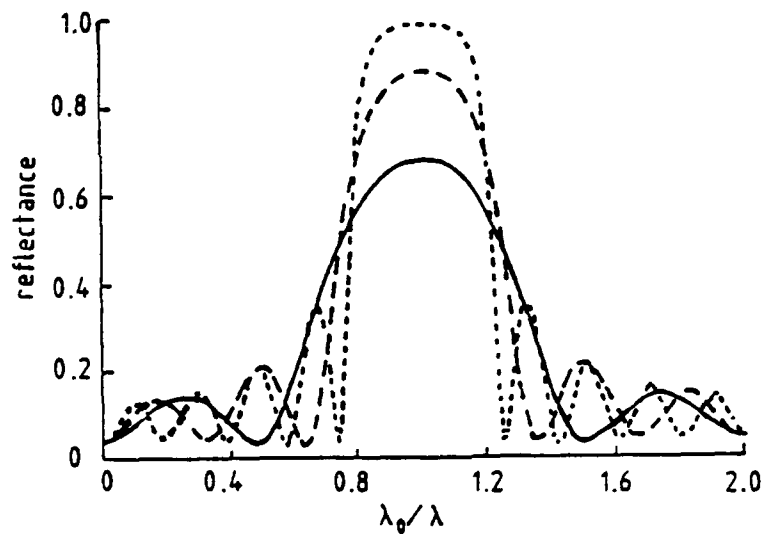


Figure 24 Computed spectral reflectance of periodic quarterwave layer reflector of ZnS ($n_H = 2.35$) and magnesium fluoride ($n_L = 1.38$) deposited on glass ($n_S = 1.52$). $n_0 = 1.00$. Full curve, three layers; broken curve, five layers; dotted curve, nine layers.

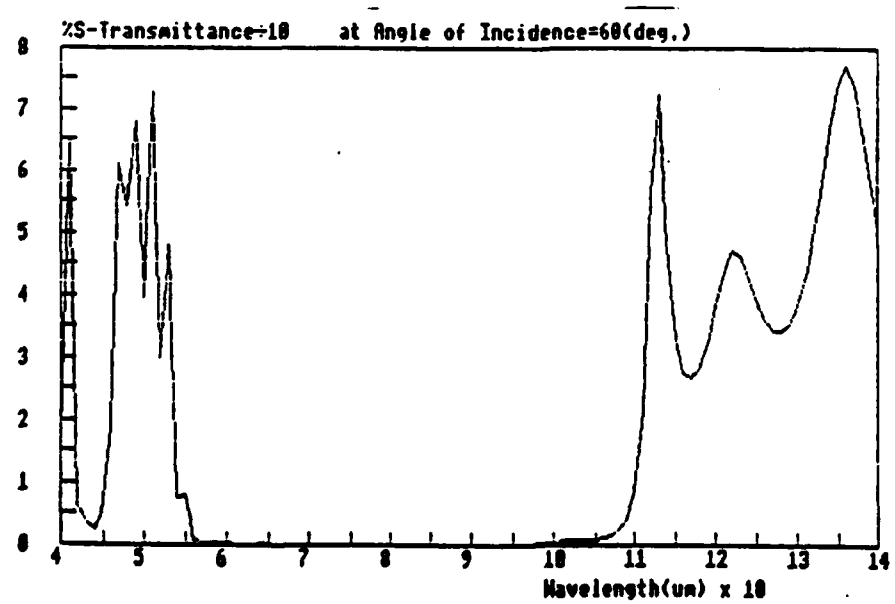
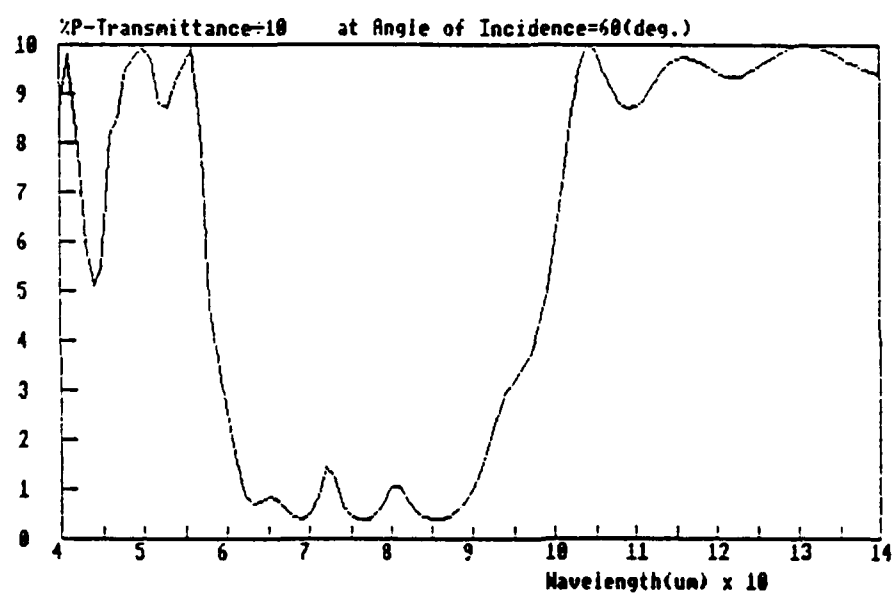
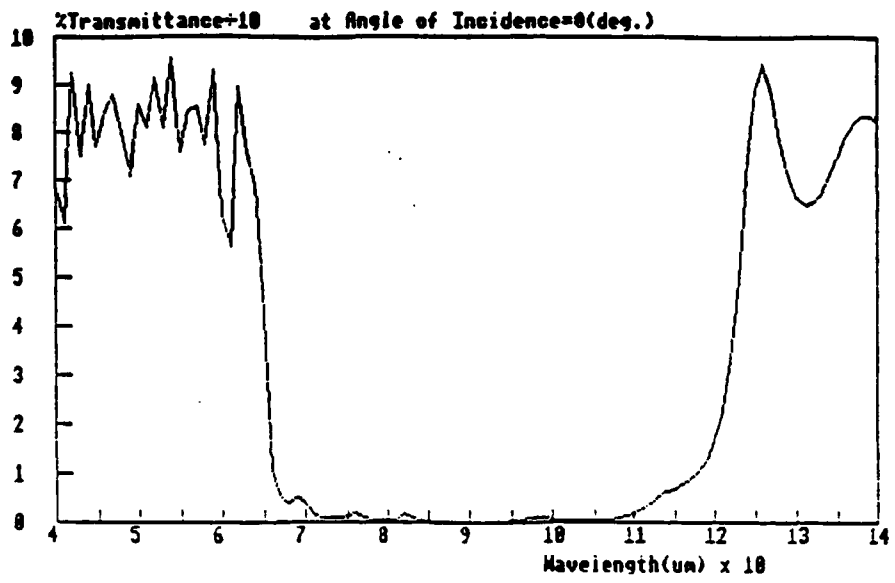


Figure 25 Spectral response of a dielectric mirror deposited on an uncoated glass substrate

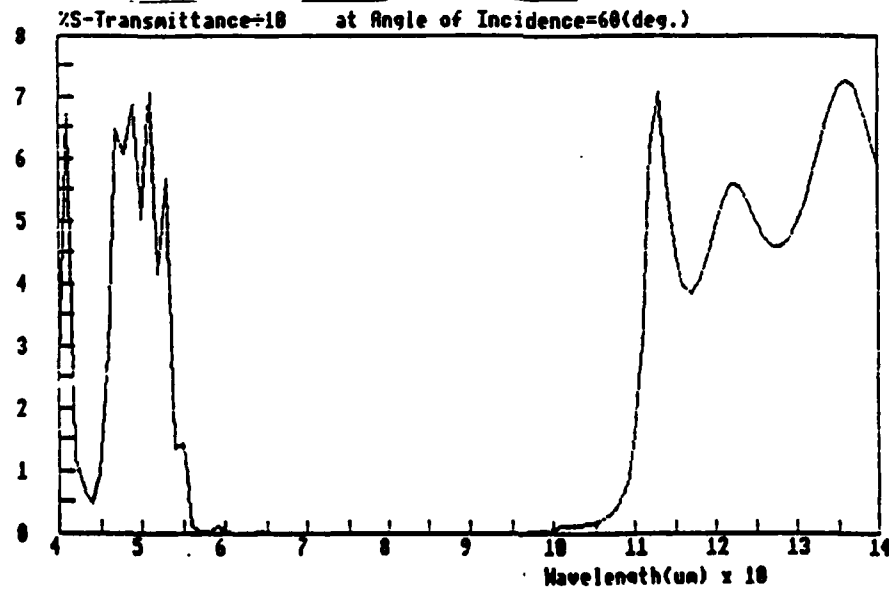
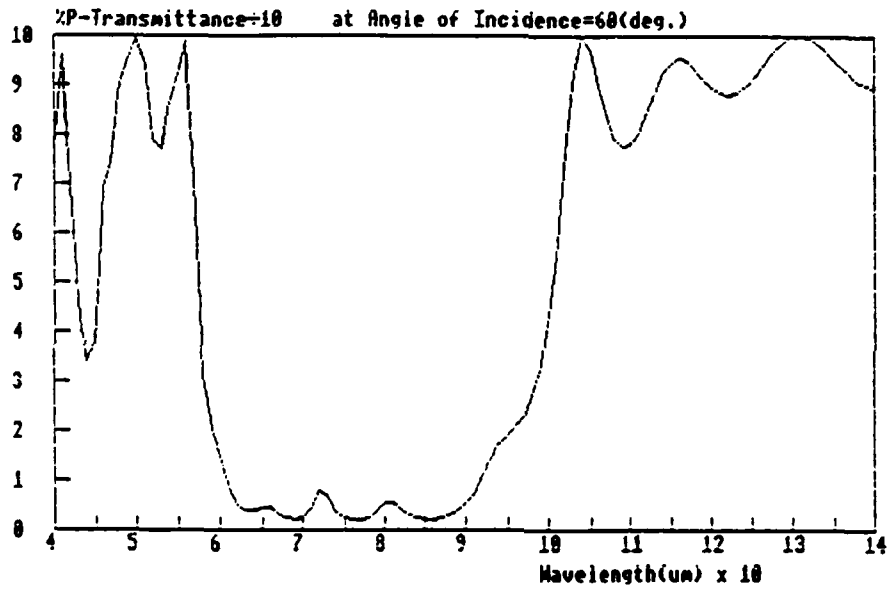
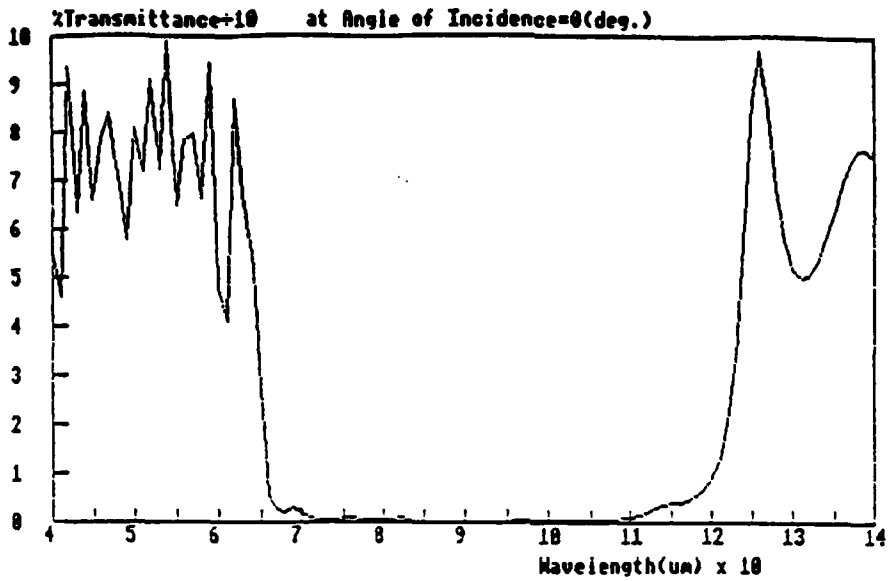


Figure 26 Spectral response of a dielectric mirror deposited on a coated (both surfaces) glass substrate

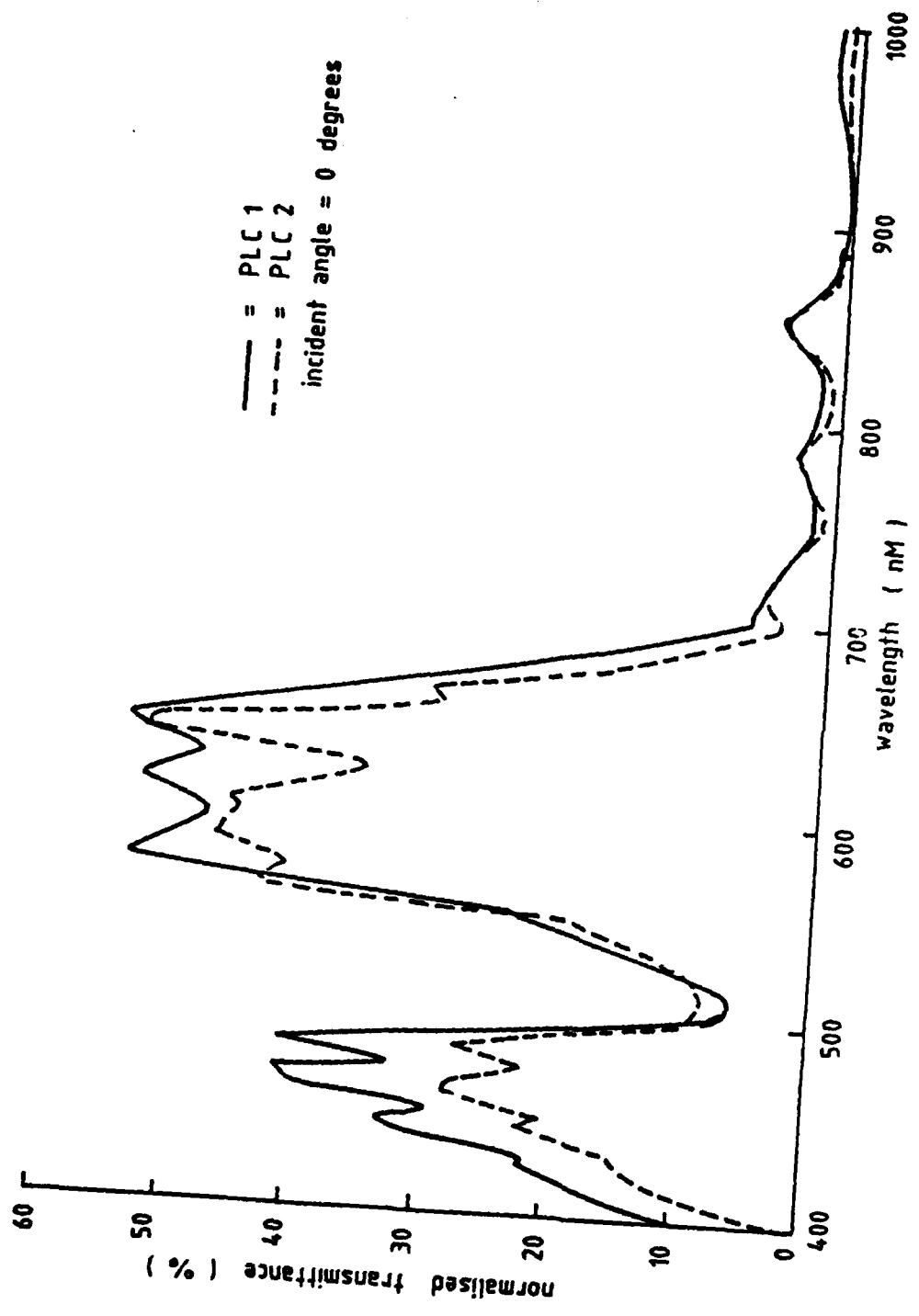


Figure 27 Normalised transmittance of optical filter on Polycarbonate substrate .

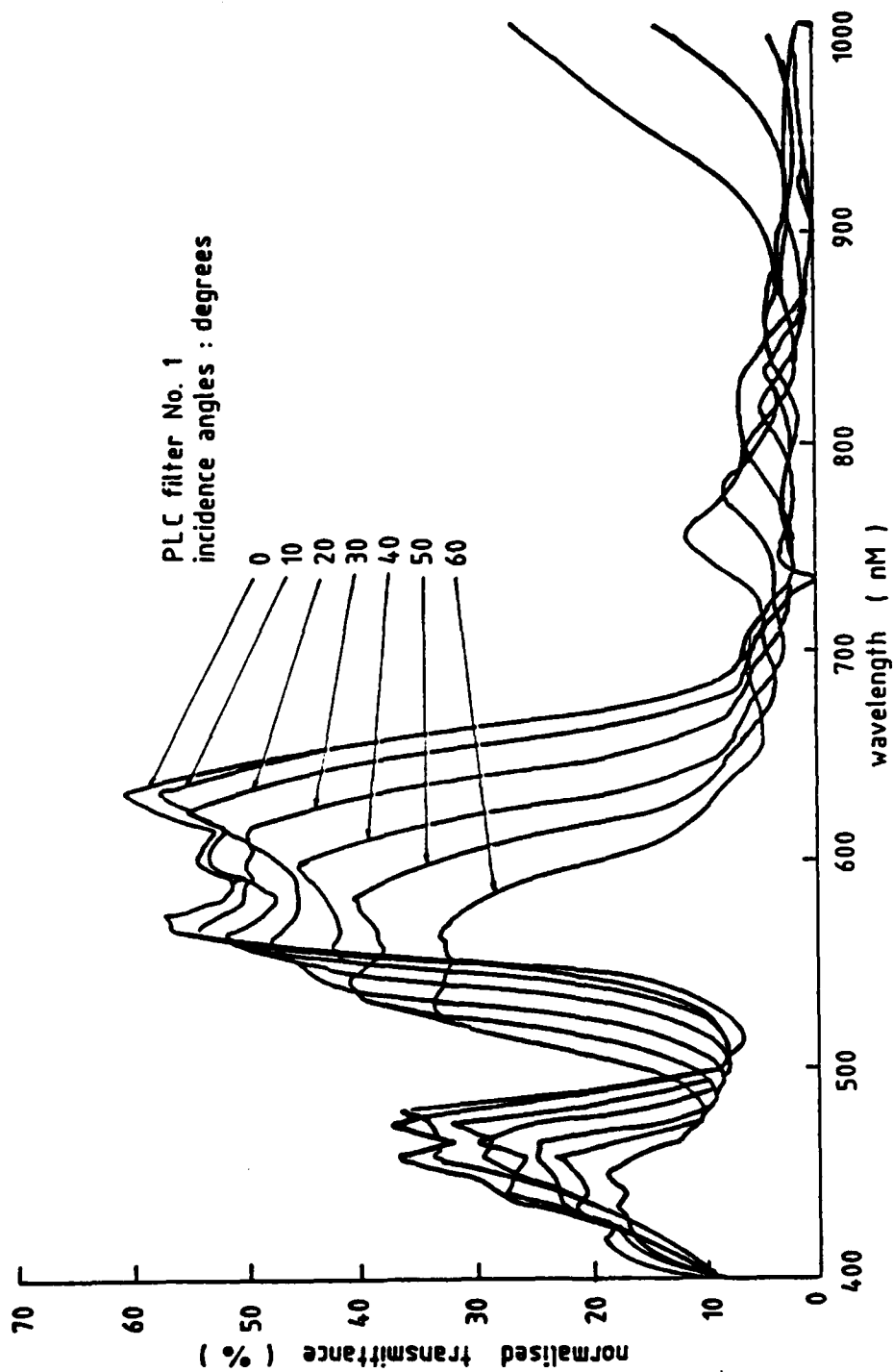


Figure 28 Normalised transmittance (at different incident angles) of optical filter on Polycarbonate substrate.

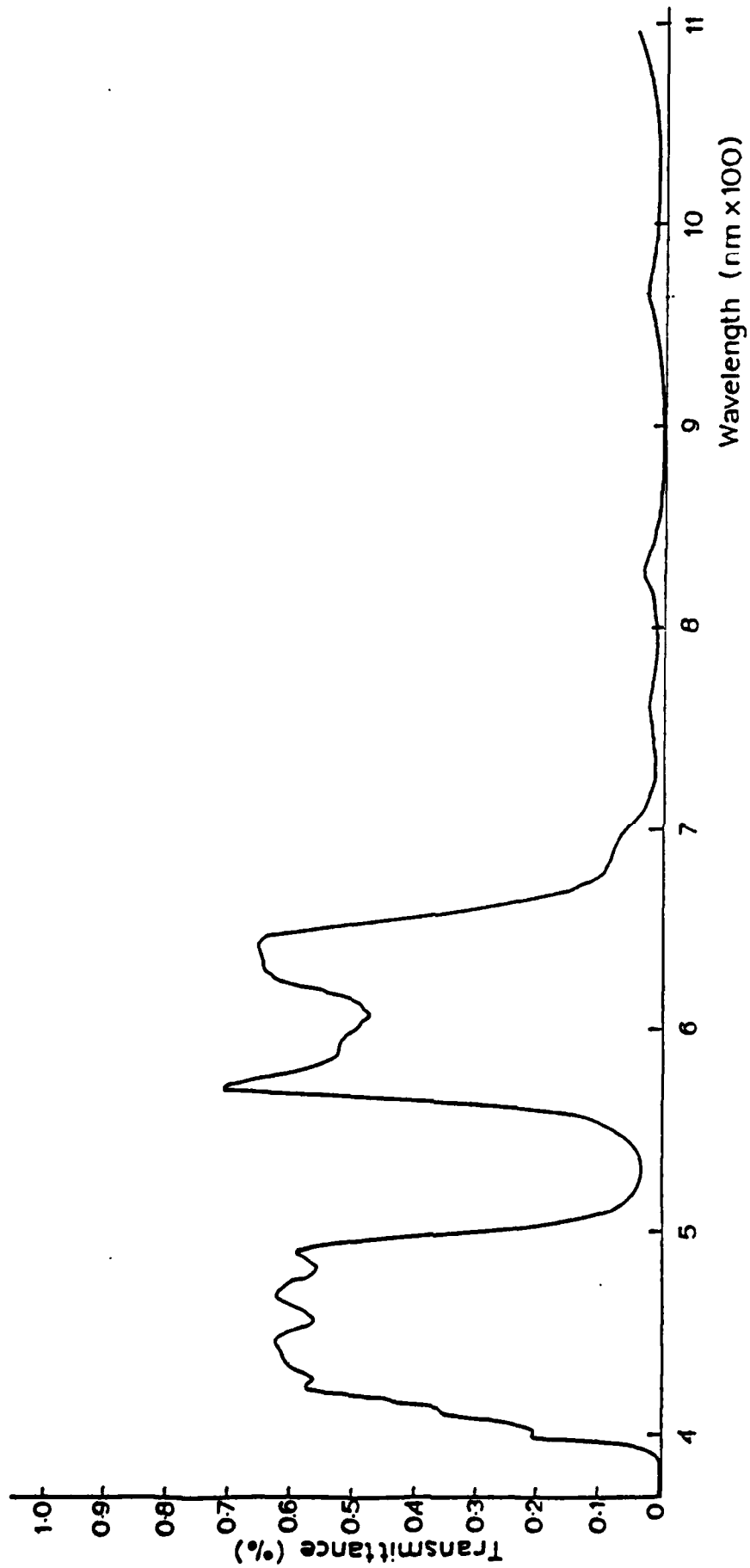


Figure 29 Transmission characteristic of Notch and Block filter at normal incidence.

Size: - 50mm x 50mm x 3mm Polycarbonate substrate.

Specification:-

(i) $T < 0.05$ for $680 < \lambda < 110$ nm and 532nm.

(ii) $T > 0.5$ for 410-500nm and 560-640nm.

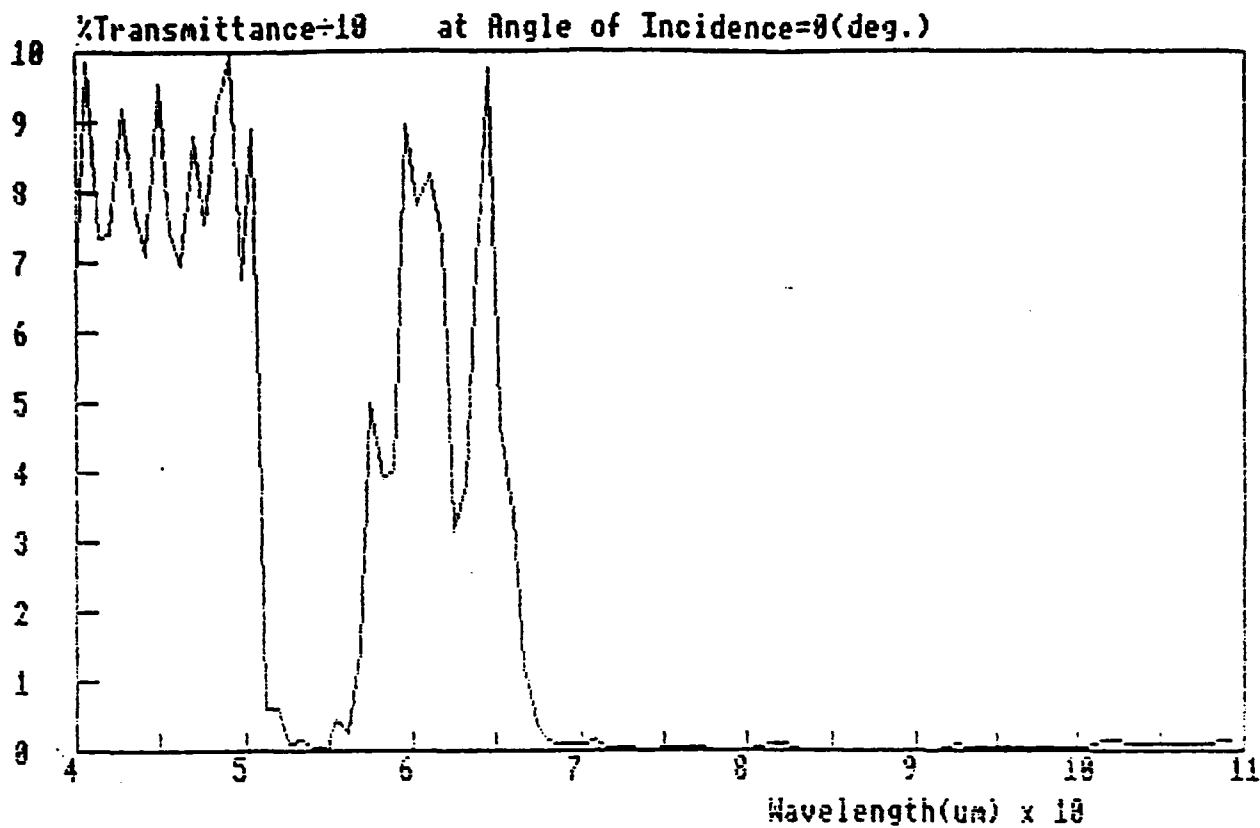


Figure 30: Transmission characteristic of the Dielectric Mirror deposited on one surface of a polycarbonate substrate (size: 50mm x 50mm x 3mm)

WA (um)	TP
0.6400	0.7935
0.6500	0.5874
0.6600	0.3150
0.6700	0.0602
0.6800	0.0157
0.6900	7.23-03